Government of Western Australia

Department of **Mines, Industry Regulation and Safety**

REPORT 186

BUILDING THE ARCHEAN CONTINENTAL CRUST: 300 Ma OF FELSIC MAGMATISM IN THE YALGOO DOME (YILGARN CRATON)

by F Clos, R Weinberg, and I Zibra

Geological Survey of Western Australia

MONASH University

Government of **Western Australia**
Department of **Mines, Industry Regulation and Safety**

REPORT 186

BUILDING THE ARCHEAN CONTINENTAL CRUST: 300 Ma OF FELSIC MAGMATISM IN THE YALGOO DOME (YILGARN CRATON)

by

F Clos*, R Weinberg* and I Zibra

* School of Earth, Atmosphere and Environment, Monash University, Clayton VIC 3800, Australia

PERTH 2018

Geological Survey of Western Australia

REFERENCE
The recommended reference for this publication is:
Clos, F, Weinberg, R and Zibra, I 2018, Building the Archean continental crust: 300 Ma of felsic magmatism in the Yalgoo dome (Yilgarn Craton): Geological Survey of Western Australia, Report 186, 23p.

ISBN 978-1-74168-816-0

A catalogue record for this book is available from the National Library of Australia

Grid references in this publication refer to the Geocentric Datum of Australia 1994 (GDA94). Locations mentioned in the text are referenced using Map Grid Australia (MGA) coordinates, Zone 50. All locations are quoted to at least the nearest 100 m.

Published 2018 by the Geological Survey of Western Australia
This Report is published in digital format (PDF) and is available online at <www.dmp.wa.gov.au/GSWApublications>.

Further details of geological publications and maps produced by the Geological Survey of Western Australia are available from:
Information Centre
Department of Mines, Industry Regulation and Safety
100 Plain Street
EAST PERTH WESTERN AUSTRALIA 6004
Telephone: +61 8 9222 3459 Facsimile: +61 8 9222 3444
www.dmp.wa.gov.au/GSWApublications

Cover photograph: A baffled red kangaroo observes geologists at work near Wollanoo Hill, 50 kilometres south of the town of Yalgoo, Western Australia

Contents

Abstract 1
Introduction 1
Geological setting 1
Late Archean granitic rocks 3
TTG 3
Transitional TTG 4
High-Mg granitic rocks 4
A-type granitic rocks 4
Low-Ca granitic rocks 4
Granitic groups in the Yalgoo dome 4
TTG 4
Field relationships, age and petrography 4
Geochemistry 9
Transitional TTGs 9
Field relationships, age and petrography 9
Geochemistry 9
High-Mg group: Cagacaroon Syenogranite 9
Field relationships, age and petrography 9
Geochemistry 12
A-type group: Damperwah and Seeligson Monzogranite 12
Field relationships, age and petrography 12
Geochemistry 13
Low-Ca granitic rocks 13
Field relationships, age and petrography 13
Geochemistry 13
Discussion 13
Stage 1: TTG magmatism (2970–2900 Ma) 13
Stage 2: high-Mg granitic rocks and transitional TTGs (2760–2740 Ma) 14
Origin of high-Mg granitic rocks: Cagacaroon Syenogranite 15
Origin of transitional TTGs 15
Lithospheric reworking 15
Stage 3: transitional TTG dykes (c. 2700 Ma) 17
Stage 4: post-tectonic granites (2640–2600 Ma); A-type and low-Ca granitic rocks 17
Origin of A-type granitic rocks 17
Origin of low-Ca granitic rocks 17
Lower crust delamination 17
Crustal reworking and implications for incremental formation of Archean continental crust 19
Conclusion 21
Acknowledgements 21
References 21

Figures

1. Geological map of the Yalgoo dome 2
2. Yalgoo dome map showing the distribution of granitic groups and sample locations 5
3. Field photographs of the granitic groups 8
4. Representative plots showing differences between granitic groups 10
5. Representative major and trace elements of the five granitic rock groups 11
6. Chondrite-normalized REE spider plots of the five granitic groups 12
7. Greenstones and granitic rocks relative timing of formation 14
8. Diagrams comparing the composition of transitional TTGs 16
9. Crustal reworking at 2760–2740 Ma (Stage 2) 16
10. Crustal reworking at c. 2700 Ma (Stage 3) 18
11. A-type discrimination diagram 18
12. Crustal reworking at 2640–2600 Ma (Stage 4) 19
13. Distribution of the three phases of crustal reworking in Youanmi Terrane 20

Tables

1. Comparison of granitic rock nomenclature in different cratons 3
2. Average major and trace element data for granitic rocks in the Yalgoo dome 6

Appendix

Granite geochemical analyses ..... available on the accompanying ZIP file

Provided with permission of David Champion, Geoscience Australia

Building the Archean continental crust: 300 Ma of felsic magmatism in the Yalgoo dome (Yilgarn Craton)

by

F Clos[1], R Weinberg[1] and I Zibra

Abstract

The evolution of granitic magmatism in the Yalgoo dome of the Yilgarn Craton offers a singular perspective on the processes needed to build felsic continental crust, because the dome exposes all five felsic intrusive groups that typify late Archean terranes. These five groups can be correlated with three major phases of juvenile magmatism and greenstone formation, culminating in four stages of magmatic activity. Phase 1 includes 2970–2900 Ma rocks of the TTG series and coeval greenstones (Stage 1). Following a magmatic hiatus of c. 100 Ma, the start of Phase 2 was marked by eruption of voluminous greenstones of the Norie and Polelle Group at 2825–2760 Ma. Thermal insulation of the crust caused reheating and softening of the crust and its underlying metasomatized mantle, resulting in a short crustal reworking episode (<20 Ma) recorded by the diapiric intrusion of 2760–2740 Ma transitional TTGs and high-Mg granitic rocks (Stage 2). Phase 3 of crustal reworking is associated with the onset of orogenic events in the Murchison Domain and resulted in the intrusion of transitional TTG dykes at c. 2700 Ma during regional east–west shortening (Stage 3). Phase 3 was followed by post-orogenic and post-volcanic A-type and voluminous low-Ca granitic rocks (Stage 4). The secular change in major and trace element chemistry of granitic rocks records a c. 300 Ma period of crustal evolution (from TTGs to low-Ca granitic rocks) and reflects progressive modification of the melting source, from basaltic to granitic, and from deep to shallow. The evolution of the Yalgoo dome ended by c. 2600 Ma and reflects the process of stabilization of continental crust through intermittent episodes of enhanced mantle activity and extensive crustal reworking.

KEYWORDS: Archean, continents, crustal evolution, geochemistry, granitic rocks

Introduction

The Archean geological record represents one-third of Earth's history, during which about 70% of the present-day volume of continental crust was formed (Taylor and McLennan, 1995; Dhuime et al., 2012, 2015; Guitreau et al., 2012). Despite post-Archean reworking of most Archean terranes, 35 large crustal blocks and minor slivers preserve information about crustal processes on early Earth (Bleeker, 2003). The crust evolved from a more mafic bulk composition before c. 3000 Ma, to an intermediate bulk composition by c. 2500 Ma (Keller and Schoene, 2012; Dhuime et al., 2012, 2015; Tang et al., 2016). This time interval corresponds with the global transition from dominant tonalite–trondhjemite–granodiorite (TTG) to potassic magmatism (Moyen, 2011; Laurent et al., 2014) and was associated with a fivefold increase in the mass of the upper continental crust due to the addition of granitic rocks (Tang et al., 2016). Bulk rock chemistry (Moyen, 2011; Laurent et al., 2014) together with Hf isotope studies (Amelin et al., 2000; Griffin et al., 2004; Davis et al., 2005; Zhang et al., 2006; Ivanic et al., 2012) and U–Pb geochronology on granitic rocks document this transition and arguably demonstrate that the Archean continental crust evolved through phases of juvenile mafic–ultramafic magmatism (i.e. greenstones) followed by episodes of crustal reworking (Campbell and Hill, 1988).

The Yalgoo dome offers a unique view on the fundamental processes necessary to generate felsic continental crust because all five felsic magmatic groups that typify late Archean terranes outcrop in the dome and in its immediate surroundings. Our new data collection of bulk rock chemistry identifies five magmatic groups, ranging (with decreasing age) from 1) TTGs to; 2) transitional TTGs; and 3) high-Mg granitic rocks post-dated by; 4) A-type; and 5) low-Ca granitic rocks. These granitic rocks are typically distributed throughout cratons and are rarely found in the same crustal section. Thus, the Yalgoo dome records the magmatic evolution of the same lithospheric column over a time span of more than 300 Ma, which enables identification of the main processes needed to build felsic continental crust by the end of the Archean.

In this contribution, we investigate the geochemical evolution recorded in these five groups to propose a four-stage tectono-magmatic evolution model linking their petrogenesis with three main pulses of mafic–ultramafic juvenile mantle inputs that may account for the diversity of late Archean granitic rocks in the Yalgoo dome. Over 300 Ma of felsic magmatism in the Yalgoo dome reflects, within a single domal structure, the crustal processes that were crucial to building Archean crust.

Geological setting

The Murchison Domain is part of the Youanmi Terrane of the Archean Yilgarn Craton (Cassidy et al., 2006; Fig. 1) and includes 2960–2720 Ma greenstone successions and

[1] School of Earth, Atmosphere and Environment, Monash University, Clayton VIC 3800, Australia

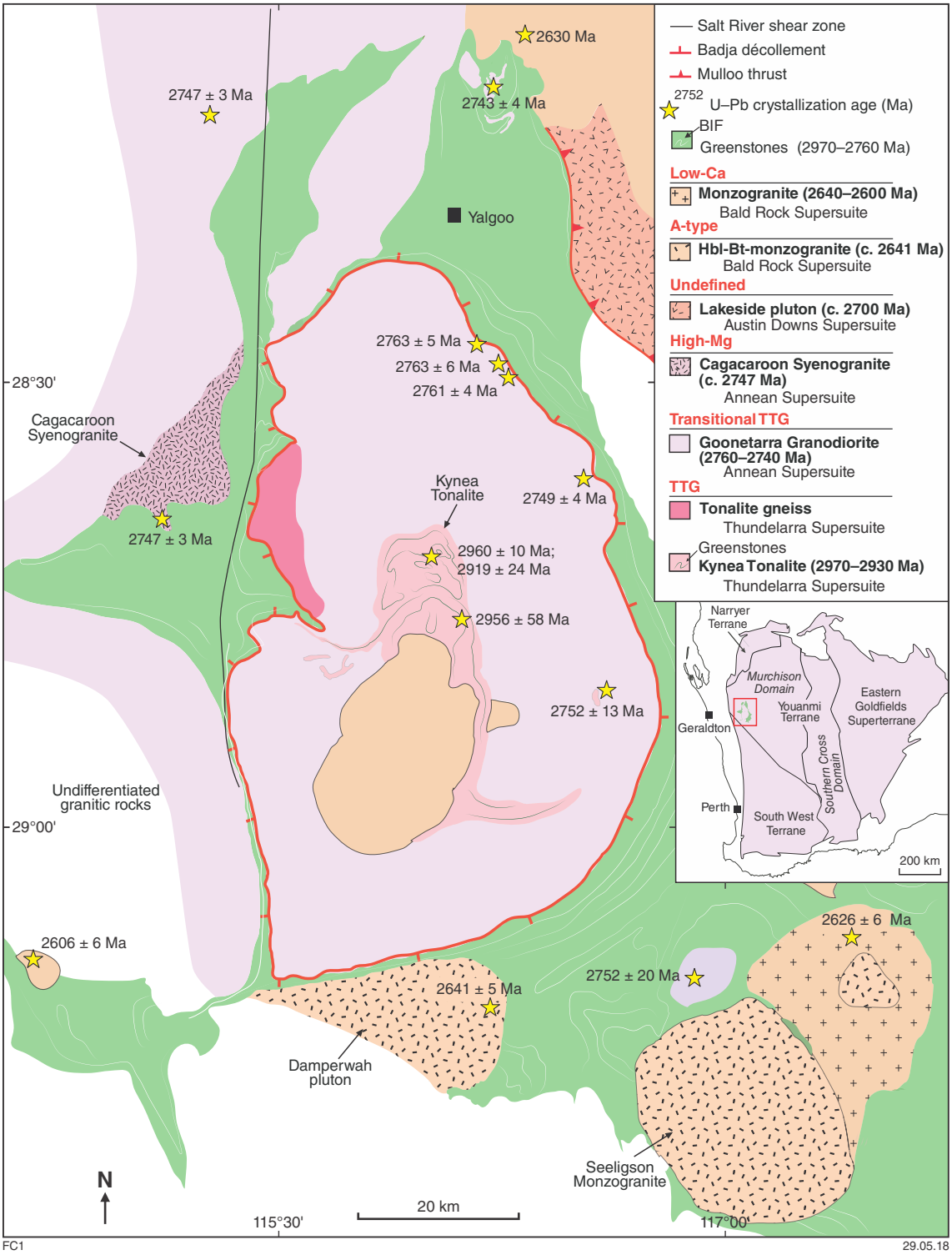

Figure 1. **Geological map of the Yalgoo dome and surrounding greenstones. Inset at centre right shows the location of the studied area in the Murchison Domain of the Youanmi Terrane, in the western Yilgarn Craton. The batholith comprises multiple generations of granitic rocks intruded over a time span >300 Ma. Yellow stars indicate the locations of U–Pb samples; zircon crystallization ages are quoted with 95% uncertainties (see text for citations)**

2970–2600 Ma granitic rocks (Van Kranendonk et al., 2013). Most of the Youanmi Terrane is dissected by a craton-scale network of transpressive shear zones and syntectonic plutons that accommodate regional east–west shortening (Zibra et al., 2014a). The three main syntectonic plutons are the 2730–2710 Ma Yarraquin pluton (Zibra et al., 2017a), the 2710–2695 Ma Lakeside pluton (Zibra et al., 2014a) and the 2680–2660 Ma Cundimurra pluton (Zibra et al., 2014b). Together, they show c. 70 Ma of nearly continuous magmatic activity, during which a north-trending magmatic to high-temperature solid-state fabric developed during crystallization. Elongated granite–greenstone patterns are truncated by a series of undeformed, post-tectonic, subcircular granitic intrusions emplaced between 2640 and 2600 Ma and known as the Bald Rock Supersuite (Ivanic et al., 2012; Van Kranendonk et al., 2013).

Significantly, the shear zones that dominate the main regional grain in the eastern parts of the Murchison Domain are absent in the westernmost part, where the Yalgoo dome is exposed. Unlike the elongated plutons in the east, this dome is a prominent 100 km long × 50 km wide elliptical granite dome enveloped by greenstone belts, comparable to the broad domes of the Paleoarchean East Pilbara Terrane (e.g. Collins, 1989). Greenstone belts wrapping around the Yalgoo dome include the 2963–2958 Ma Gossan Hill Formation comprising felsic volcanic and volcaniclastic rocks, unconformably overlain by mafic volcanic rocks, felsic volcanoclastic sandstones and banded iron-formation of the 2825–2805 Ma Norie Group (Van Kranendonk et al., 2013). On top of the Norie Group lies the up to 8 km thick 2800–2760 Ma Polelle Group, a continuous volcanic succession ranging from komatiitic basalt to tholeiitic basalt and minor andesite (Ivanic et al., 2015). These rocks are unconformably overlain by the Mougooderra Formation, a siliciclastic succession containing felsic volcanic rocks dated at 2758 ± 4 Ma (GSWA ID 211101) and present only in the Yalgoo dome area (Ivanic et al., 2015). The dome itself is composed of several 2760–2600 Ma granitic intrusions that are progressively younger and compositionally more evolved towards the centre of the dome (Goonetarra Granodiorite in Fig. 1; Zibra et al., 2017b). Breaking this general younging trend, the oldest rocks outcrop in the core of the dome forming a well-exposed region, approximately 8 × 12 km in size (Fig. 1). This unit comprises 2970–2900 Ma migmatitic Kynea Tonalite interlayered with remnants of amphibolite and banded iron-formation (Myers and Watkins, 1985), intruded by a north-trending, subvertical swarm of granitic dykes dated at c. 2700 Ma (Zibra et al., 2017b).

Late Archean granitic rocks

Archean terranes are dominated by voluminous suites of TTG rocks (~50%), greenstones (~30%) and K-rich granitic rocks (<20%; Condie, 1993). Although potassic granitic rocks are a minor constituent of Paleoarchean to Mesoarchean terranes, they become more widespread towards the end of the Archean, representing the last magmatic episode in every Archean craton (Condie, 1993). The classification scheme proposed in this work is based on the original granitic groups identified in the Yilgarn Craton by Champion and Sheraton (1997), but with a revised nomenclature. Following Champion and Smithies (2001), we subdivided the high-Ca group of Champion and Sheraton (1997) into a TTG (K_2O/Na_2O <0.6) and a transitional TTG group (K_2O/Na_2O>0.6 and high large-ion lithophile element [LILE], U, Th content), both distinguished by a strong heavy rare earth element (HREE) depletion. The mafic and the high-high field strength element (HFSE) groups of Champion and Sheraton (1997) are renamed 'high-Mg' and 'A-type', respectively (Table 1).

TTG

The term 'TTG' as used here refers to the high-Al TTG classification of Barker and Arth (1976). In all preserved Archean cratons, these granitic suites represent the first preserved evidence of felsic continental crust (Champion and Smithies, 2007; Laurent et al., 2014). These rocks show internal variations, but invariably comprise Al-rich and Na-rich granitic rocks with marked HREE, Nb-Ta-Ti depletions and variable Sr enrichments (Barker and Arth, 1976). After more than 40 years of research (see review of Moyen and Martin, 2012), there is consensus that the diagnostic trace element geochemistry of TTGs is produced by partial melting of a hydrous mafic parent with variable proportions of garnet, amphibole, plagioclase and rutile left behind in the restite (Martin, 1987).

Table 1. Comparison of nomenclature between the Yilgarn Craton, Murchison Domain, other Archean terranes and this work

Yilgarn Craton[1]	*Murchison Domain*[2]	*Other terranes*[3]	***This work***
High-Ca	-	TTG	**TTG**
High-Ca	Cullculli, Big Bell	Medium-K, hybrid	**Transitional TTG**
Mafic	Cullculli	Sanukitoid high-Mg diorites	**High-Mg**
High-HFSE	Eelya	A-type	**A-type**
Low-Ca	Walganna and Wogala	High-K, potassic, biotite-muscovite granite	**Low-Ca**

NOTES: 1 Champion and Sheraton, 1997
2 Ivanic et al., 2012
3 Heilimo et al., 2010; Moyen, 2011; Farina et al., 2015; Laurent et al., 2014

Transitional TTG

The term 'transitional TTG' was introduced by Champion and Smithies (2001) to describe a group of granitic rocks identified in the Yilgarn and Pilbara Cratons and characterized by broadly TTG-like compositions, but marked by further LILE, Th and U enrichment (Champion and Sheraton, 1997; Champion and Smithies, 2007). These rocks are found in many other Archean terranes worldwide, including the Tanzania Craton (Opiyo-Akech et al., 1999), western Dharwar Craton (Prabhakar et al., 2009), Karelian Province (Mikkola et al., 2012), Amazonia Craton (Almeida et al., 2010), Kaapvaal Craton (Laurent et al., 2014) and São Francisco Craton (Farina et al., 2015), and commonly post-date the main TTG phase — except in the Wyoming Province, where they are apparently coeval with TTG (Frost et al., 2006). In most provinces, transitional TTGs make up 10–15% of the granitic rocks, but in the Yilgarn Craton (Champion and Sheraton, 1997) and the Wyoming Province they make up >60% of the total. Transitional TTGs have previously been referred to as hybrid granitic rocks (Laurent et al., 2014), high-Ca granitic rocks (Champion and Sheraton, 1997), medium-K granitic rocks (Farina et al., 2015), TTG sensu lato (Mikkola et al., 2012) and high Ba-Sr granitic rocks (Peng et al., 2013).

High-Mg granitic rocks

High-Mg granitic rocks are defined by an enigmatic geochemical signature with high contents of compatible elements (MgO, Ni, Cr and V) and a noticeable enrichment in LILEs (Defant and Drummond, 1990; Rapp et al., 1999; Smithies and Champion, 2000). In late Archean terranes, granitic rocks with similar compositions were collectively grouped as high-Mg diorites (Smithies and Champion, 2000) or Archean sanukitoids (Shirey and Hanson, 1984; Smithies and Champion, 2000; Heilimo et al., 2010; Laurent et al., 2014) based on geochemical similarities with Miocene high-Mg andesites from the Setouchi volcanic belt in Japan (sanukites of Tatsumi and Ishizaka, 1981).

A-type granitic rocks

A-type granitic rocks are felsic rocks rich in FeO_T, K_2O, P_2O_5, TiO_2 and HFSE with moderately fractionated rare earth element (REE) patterns and marked negative Eu–Sr anomalies (Whalen et al., 1987; Frost and Frost, 2011). Compositionally similar granitic rocks are considered to be post-collisional in most Proterozoic (Duchesne et al., 2010) and Neoarchean terranes, including the Yilgarn Craton, where they are known as high-HFSE granitic rocks (Champion and Sheraton, 1997).

Low-Ca granitic rocks

Granitic rocks of the low-Ca group form post-tectonic intrusions (biotite monzogranite and syenogranite) that truncate older granite and greenstones (Champion and Sheraton, 1997) between 2640 and 2600 Ma (Van Kranendonk et al., 2013). These intrusions are defined by high K_2O/Na_2O ratio, low Al_2O_3 and Sr content along with moderately fractionated REE patterns, with large negative Eu anomalies (Champion and Sheraton, 1997; Laurent et al., 2014). In other cratons they are referred as high-K granitic rocks (Whalen et al., 2004; Almeida et al., 2010; Farina et al., 2015) or biotite-muscovite granitic rock (Laurent et al., 2014).

Granitic groups in the Yalgoo dome

In this section, we describe the geology, petrography and geochemistry of the five granitic rock groups that outcrop within the Yalgoo dome and in two plutons in the immediate surrounding area (Fig. 2). This study is based on 149 whole-rock analyses: 92 analyses are from the Geological Survey of Western Australia (GSWA) database and 57 are from Geoscience Australia (GA). All analyses can be found in the Appendix (see accompanying ZIP file). The average compositions of each granite group are presented in Table 2. All ages reported here reflect the age of the protolith and were obtained by SHRIMP U–Pb analyses on zircons according to the GSWA standard. The geochronology data can be found in the Compilation of geochronology information 2016 (GSWA, 2016).

TTG

Field relationships, age and petrography

TTGs belong to the Thundelarra Supersuite (Zibra et al., 2017b) and are present in two distinct structural domains: in the migmatitic core of the Yalgoo dome and along the northwest flank of the dome (Fig. 3). Rocks in the core include migmatitic tonalite intruded into an older metamorphosed greenstone succession comprising amphibolite and banded iron-formation that now forms remnants inside the complex (Myers and Watkins, 1985; Fenwick, 2014). Wiedenbeck and Watkins (1993) report mainly very discordant U–Pb dates that average c. 2.9 Ga from zircon cores (sample GSWA 83339) and 2.8 – 2.7 Ga from zircon rims, interpreted as the crystallization age of the protolith and an overgrowth linked to migmatization, respectively (Fig. 3a). More recent investigations of rocks of the Yalgoo dome further constrain the age range of the protolith to 2960 ± 10 Ma (GSWA 209689, Lu et al., 2017) and c. 2.95 Ga (GSWA 155879, Wingate et al., 2015a).

The TTGs in the core of the dome consist of biotite-rich, grey tonalite gneiss with a pervasive solid-state foliation delineated by preferential alignment of biotite. These gneisses have a well-developed migmatitic layering (Fig. 3a) and the fraction of leucocratic material is variable, resulting in a heterogeneous appearance. Layering is defined by alternations of mesosome and leucosome. The mesosome comprises abundant plagioclase, quartz and interstitial K-feldspar and accessory titanite and epidote. Biotite is the dominant ferromagnesian mineral and is commonly partially replaced by chlorite. Leucosomes exhibit the same mineralogy as mesosomes, but with a net decrease in biotite and an increase in K-feldspar content.

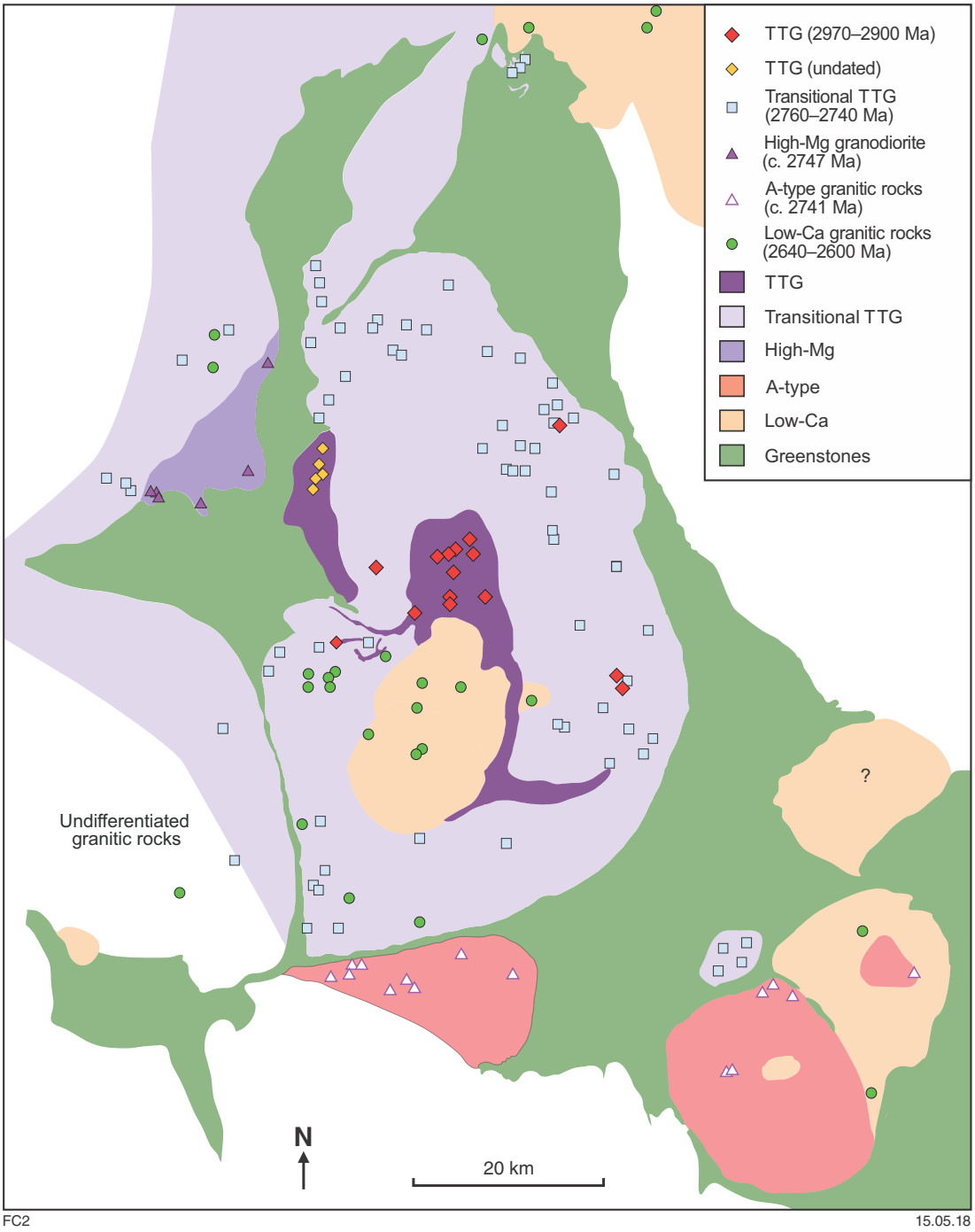

Figure 2. Yalgoo dome map showing the locations of whole-rock geochemical analyses (see Appendix) and distribution of the five groups of granitic rocks

Table 2. Average major and trace element data for granitic rocks in the Yalgoo dome. All Fe as FeO_T

Name Suite Age (Ma)	*Units*	*Kynea Tonalite TTG 2970–2930*	*SD*	*Tonalite gneiss TTG*	*SD*	*Goonetarra Granodiorite Transitional TTG 2760–2740*	*SD*	*Dykes Transitional TTG 2707–2700*	*SD*	*Cagacaroon Syenogranite High-Mg 2747*	*SD*	*Damperwah and Seeligson A-type 2641*	*SD*	*Post-tectonic granitic rocks Low-Ca 2640–2600*	*SD*
SiO_2	(%)	71.93	1.33	70.76	2.41	72.20	1.48	72.56	2.05	63.28	2.42	70.89	1.25	73.48	1.84
TiO_2	(%)	0.23	0.09	0.28	0.11	0.20	0.07	0.12	0.03	0.66	0.13	0.48	0.14	0.20	0.11
Al_2O_3	(%)	15.13	0.52	15.37	0.50	14.81	0.57	15.31	1.13	14.35	0.79	13.27	0.36	13.58	0.53
FeO_T	(%)	1.87	0.43	2.81	1.31	1.59	0.51	1.11	0.26	4.91	0.86	3.79	0.78	1.61	0.64
MgO	(%)	0.51	0.20	0.68	0.35	0.40	0.15	0.17	0.02	2.91	0.74	0.37	0.07	0.28	0.16
CaO	(%)	2.06	0.33	3.03	0.78	1.72	0.41	1.60	0.37	3.70	0.68	2.26	0.60	1.07	0.37
Na_2O	(%)	4.81	0.42	4.66	0.39	4.29	0.40	4.44	0.41	3.51	0.11	3.10	0.19	3.42	0.36
K_2O	(%)	2.57	0.67	1.65	0.33	3.64	0.65	4.10	1.46	4.45	0.58	4.06	0.36	4.91	0.54
P_2O_5	(%)	0.08	0.03	0.08	0.03	0.07	0.03	0.04	0.01	0.40	0.07	0.14	0.06	0.07	0.05
MnO	(%)	0.03	0.02	0.04	0.01	0.05	0.03	0.01	0.00	0.11	0.04	0.09	0.04	0.06	0.04
LOI	(%)	0.38	0.14	0.47	0.25	0.71	0.46	0.31	0.05	0.81	0.40	0.85	0.68	0.99	0.77
Total	(%)	99.61	0.47	99.84	1.04	99.68	0.39	99.76	0.39	99.09	0.34	99.24	0.33	99.63	0.16
Ba	(ppm)	1133.28	488.16	517.36	234.08	1557.52	563.77	2244.43	1150.68	2353.87	283.36	1604.22	264.20	717.37	313.33
Ce	(ppm)	63.27	36.63	40.65	9.80	64.16	25.33	51.23	19.67	119.20	17.19	233.28	144.48	117.20	62.24
Co	(ppm)	30.65	25.09	36.22	49.53	37.09	29.90	15.40	23.13	36.23	14.67	11.73	12.81	13.53	27.77
Cr	(ppm)	76.57	73.20			11.79	34.17	102.00	23.45	102.67	54.81	62.70	86.57	12.56	46.55
Cs	(ppm)	8.43	12.87	3.48	3.11	3.29	2.76	3.57	3.01	7.08	5.24	3.60	1.35	5.77	3.12
Cu	(ppm)	5.06	4.80	4.26	3.80	5.49	11.17	3.14	2.27	18.27	9.22	7.39	3.54	3.25	2.62
Dy	(ppm)	0.87	0.43	1.19	0.80	0.91	0.39	0.59	0.11	3.48	0.59	9.27	1.44	4.39	2.25
Er	(ppm)	0.39	0.17	0.64	0.52	0.43	0.22	0.30	0.08	1.61	0.19	5.24	1.10	2.54	1.33
Eu	(ppm)	0.64	0.26	0.71	0.21	0.65	0.18	0.60	0.11	1.95	0.29	2.77	0.54	0.55	0.25
Ga	(ppm)	20.70	2.04	20.12	0.46	18.70	2.13	18.08	1.15	17.76	1.17	19.10	2.03	18.61	1.21
Gd	(ppm)	1.53	0.84	1.88	0.83	1.66	0.58	0.97	0.16	5.72	0.92	10.93	1.37	5.05	2.41
Ge	(ppm)	0.63	0.11	0.75	0.13	0.82	0.18	0.53	0.05	1.16	0.27	1.46	0.16	1.24	0.15
Hf	(ppm)	3.87	0.85	4.10	0.73	3.62	0.79	3.22	0.80	5.51	1.03	12.10	1.11	5.42	1.86
Ho	(ppm)	0.16	0.08	0.31	0.17	0.17	0.09	0.10	0.03	0.58	0.08	1.84	0.33	0.87	0.47
In	(ppm)	0.02	0.01	0.02	0.01	0.01	0.00	0.01	0.00	0.03	0.00	0.09	0.01	0.03	0.01
La	(ppm)	41.63	26.09	24.47	5.53	38.65	15.31	24.77	6.12	71.57	11.98	118.40	69.50	62.03	32.31
Li	(ppm)	65.19	61.45	18.32	7.95	21.39	13.92	11.50	6.31	20.53	10.99	27.99	11.89	35.89	18.35
Lu	(ppm)	0.07	0.03	0.15	0.08	0.08	0.05	0.03	0.01	0.23	0.04	0.72	0.21	0.36	0.16
Mo	(ppm)	1.28	2.32	0.10	0.00	0.28	0.28	1.10	0.83	1.67	1.17	1.75	1.44	0.59	0.54
Nb	(ppm)	4.06	2.27	5.36	1.83	4.73	2.62	1.92	0.53	8.38	1.59	19.78	2.92	17.44	7.80

Table 2. continued

Name Suite Age (Ma)	*Units*	*Kynea Tonalite TTG 2970–2930*	*SD*	*Tonalite gneiss TTG*	*SD*	*Goonetarra Granodiorite Transitional TTG 2760–2740*	*SD*	*Dykes Transitional TTG 2707–2700*	*SD*	*Cagacaroon Syenogranite High-Mg 2747*	*SD*	*Damperwah and Seeligson A-type 2641*	*SD*	*Post-tectonic granitic rocks Low-Ca 2640–2600*	*SD*
Nd	(ppm)	21.07	13.91	15.15	3.08	19.54	7.48	12.30	2.13	47.28	11.01	72.04	17.21	37.06	19.57
Ni	(ppm)	7.73	8.60	8.12	7.89	4.55	1.66	2.92	1.20	59.43	31.10	7.49	8.52	3.81	2.07
Pb	(ppm)	25.79	7.94	13.76	4.28	39.03	14.14	38.30	9.54	44.15	9.34	39.43	8.08	56.54	17.37
Pr	(ppm)	6.62	4.63	4.39	1.04	6.14	2.37	3.97	0.87	13.32	2.94	19.16	5.68	11.47	6.12
Rb	(ppm)	111.54	64.97	66.80	14.84	136.67	45.19	107.95	38.59	203.30	40.91	152.71	37.51	328.25	70.54
Sm	(ppm)	2.75	1.59	2.62	0.76	2.64	0.93	1.67	0.26	7.27	1.20	12.55	1.64	6.14	2.92
Sr	(ppm)	523.02	224.99	306.74	80.94	411.61	192.98	405.33	55.89	609.92	83.46	188.79	34.00	91.95	36.77
Ta	(ppm)	0.54	0.38	0.60	0.16	0.60	0.37	0.24	0.05	0.87	0.15	1.37	0.38	1.98	0.94
Tb	(ppm)	0.22	0.10	0.32	0.16	0.20	0.09	0.11	0.01	0.71	0.09	1.75	0.21	0.80	0.41
Th	(ppm)	11.29	4.25	7.38	1.64	16.48	8.59	10.27	1.29	25.57	7.09	36.12	37.32	37.93	13.45
Tl	(ppm)	0.68	0.46	0.27	0.05	0.69	0.21	0.56	0.20	1.26	0.17	0.72	0.07	1.90	0.41
Tm	(ppm)	0.08	0.04	0.21	0.13	0.09	0.04	0.09	0.01	0.25	0.06	0.85	0.14	0.44	0.19
U	(ppm)	2.16	1.22	0.45	0.83	3.70	3.26	1.34	0.66	4.78	0.78	3.91	1.58	19.20	21.79
V	(ppm)	24.21	7.91	29.00	13.24	18.08	7.89	17.50	9.19	90.67	19.02	12.70	4.79	10.05	12.22
Y	(ppm)	4.86	2.77	6.46	4.50	5.45	4.22	3.32	0.92	17.57	2.83	53.25	10.42	30.04	19.12
Yb	(ppm)	0.32	0.17	0.54	0.45	0.39	0.22	0.27	0.08	1.41	0.18	4.77	1.16	2.42	1.21
Zn	(ppm)	45.20	13.34	49.20	8.76	32.24	8.56	24.33	7.42	61.33	11.24	84.40	18.18	37.54	12.10
Zr	(ppm)	147.73	39.12	145.40	26.73	128.00	34.75	121.50	28.76	177.17	37.41	406.93	86.25	179.13	97.76

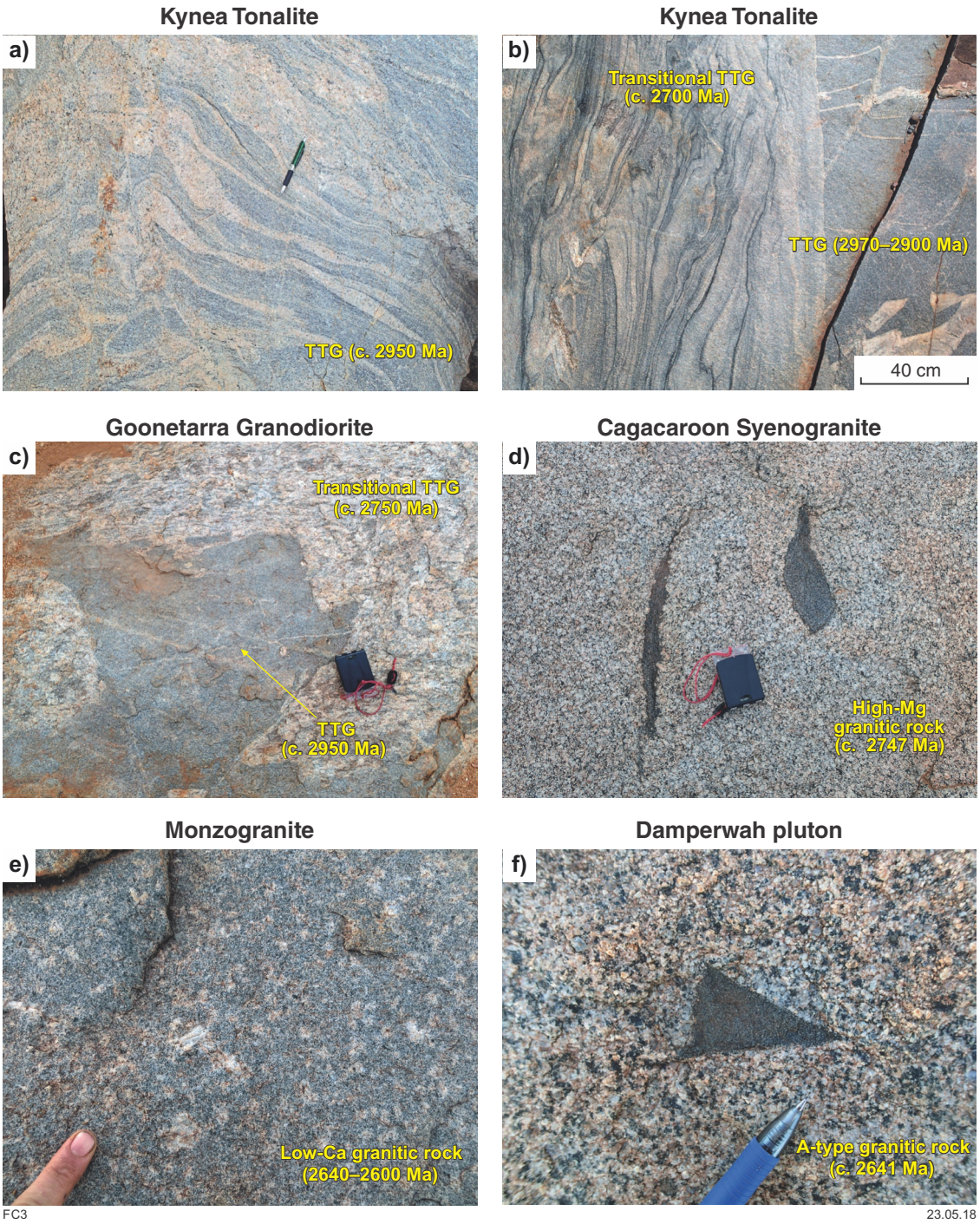

Figure 3. **Field photographs of representative examples of the diverse late Archean granitic rocks from the Yalgoo dome: a) 2970–2900 Ma Kynea Tonalite showing migmatitic structures; b) polyphase 2970–2900 Ma migmatitic Kynea Tonalite (right side) cut by c. 2700 Ma granitic dykes (left side) that contain biotite-rich schlieren and have transitional TTG compositions; c) K-feldspar-phyric Goonetarra Granodiorite (2760–2740 Ma) with transitional TTG composition containing angular xenolith of 2970–2900 Ma migmatitic tonalite; d) coarse-grained hornblende-bearing Cagacaroon Syenogranite, a high-Mg K-feldspar-phyric intrusion containing mafic enclaves rich in pyroxene and hornblende; e) coarse-grained, low-Ca monzogranite with preferred orientation of large K-feldspar porphyroclasts; f) mesocratic, equigranular A-type granitic rocks of the Damperwah pluton, containing angular enclaves of banded iron-formation; the mafic enclaves contain intergrown Fe-rich hornblende and biotite**

TTGs on the northwest side of the dome comprise an undated tonalite gneiss (Fig. 1), consisting of plagioclase, quartz, K-feldspar and biotite with accessory titanite and epidote. Primary magmatic fabrics are partially overprinted by a solid-state foliation, which varies in intensity, yet increases towards the greenstone contact in the west.

Geochemistry

TTGs in the Yalgoo dome are typical calc-alkalic to calcic, mildly peraluminous (1< A/CNK >1.1; Fig. 4b,c) and sodic granitic rocks with K_2O/Na_2O <0.6 (Fig. 5; Moyen and Martin, 2012; Laurent et al., 2014). High silica (SiO_2 >69.0 wt%) and Al_2O_3 (14.3 – 16.3 wt%) contents are associated with low ferromagnesian oxides (Table 2) and variable CaO (1.5 to 4.0 wt%) (Fig. 5). REE are strongly fractionated with a characteristic depletion in HREE on normalized trace element diagrams (Fig. 6) and La/Yb >50 for most of the samples (Fig. 4f). The undated TTGs on the northwest margin of the dome show LILE contents comparable to average Archean TTGs (Moyen, 2011; Moyen and Martin, 2012) with Sr = 236–439 ppm, Ba = 234–845 ppm, Rb = 54.9 – 92.3 ppm and low K_2O content (1.19 – 2.07 wt%) (Fig. 5). In contrast, the c. 2950 Ma TTGs in the core of the dome (Fig. 1), are characterized by a heterogeneous LILE enrichment, with higher K_2O (1.57 – 3.77 wt%), Ba (465–2242 ppm), Sr (290–1201 ppm) and Rb (71–321 ppm).

Transitional TTGs

Field relationships, age and petrography

Transitional TTGs comprise large intrusions of granodiorite and monzogranite, belonging to the Goonetarra Granodiorite (Annean Supersuite; Van Kranendonk et al., 2013). Transitional TTGs cover most of the dome (Fig. 1), with multiple intrusions of porphyritic to equigranular granitic rocks containing centimetre- to metre-sized xenoliths of 2970–2900 Ma migmatitic tonalite (Fig. 3c). The oldest intrusions crop out along the northeast margin and are dated at 2760 Ma (2763 ± 5 Ma, GSWA 214138; 2761 ± 4 Ma, GSWA 214139; 2763 ± 6 Ma, GSWA 214101; Zibra et al., 2017b). In other parts of the dome, these granitic rocks are possibly younger and vary in age down to c. 2740 Ma (2752 ± 13 Ma, GSWA 155858, Lu et al., 2017; 2752 ± 20 Ma, GA 999564016c; 2749 ± 4 Ma, GSWA 155822, Wingate et al., 2015b; 2743 ± 4 Ma, GA 999564100; 2747 ± 3 Ma, GA 999569164a) suggesting that most of the dome developed in c. 20 Ma between 2760 and 2740 Ma.

Distant from the margins, these granitic rocks exhibit a magmatic fabric marked by the preferred orientation of plagioclase and K-feldspar phenocrysts in a matrix of quartz and biotite with minor amounts of epidote, titanite and magnetite. At granite–greenstones boundaries, magmatic textures are overprinted by a high-grade solid-state foliation with steeply plunging mineral lineations and a dome-up, greenstone-down sense of motion (Foley, 1997; Zibra et al., 2017b). This foliation is concordant with the elliptical shape of the dome and parallel to the contact with the greenstones.

Younger transitional TTGs form a dyke swarm that intrudes the Kynea Tonalite in the core of the dome at 2700 Ma (2700 ± 7 Ma, GSWA 214315; 2706 ± 5 Ma, GSWA 214324; Zibra et al., 2017b) and are temporally and compositionally similar to the Big Bell Suite (Ivanic et al., 2012). Most of these dykes have granitic compositions and equigranular textures with plagioclase, K-feldspar quartz and biotite, and accessory titanite, magnetite, apatite and epidote.

Geochemistry

Transitional TTGs (2760–2740 Ma) are calc-alkalic (Fig. 4b) and mildly peraluminous (1 <A/CNK >1.1; Fig. 4c) granitic rocks with a narrow silica range (70.0 – 76.0 wt% SiO_2) and large LILE variations (Fig. 5; Table 2). They are more potassic than TTGs (Fig. 4a) and silica correlates negatively with major oxides except K_2O, which increases from 3.0 wt% (at 70.0 wt% SiO_2) up to 5.0 wt% (at 75.0 wt% SiO_2; Fig. 5). Normalized trace element patterns are like those of the TTGs, marked by depletion in HREE (Fig. 6), a negative to positive Eu anomaly (Eu*/Eu = 0.5 – 2; Fig. 4d) and a range of La/Yb ratios (17–213; Fig. 4f). As any silica content, LILE, Th and U content is significantly higher in transitional TTGs than in TTGs (Fig. 5).

The c. 2700 Ma transitional TTG dykes are chemically similar to their older counterparts except for a slightly larger range in K_2O (2.4 – 6.6 wt%), Al_2O_3 (13.7 – 16.8 wt%) and Ba (1376–4303 ppm), accompanied by an exclusively positive Eu anomaly (Eu*/Eu >1.5; Fig. 4d). Given that Ba and Eu are strongly partitioned to feldspars and that K_2O and Al_2O_3 enrichment occurs for every specimen, we infer that accumulation of K-feldspar played a key role in the scatter of the dataset.

High-Mg group: Cagacaroon Syenogranite

Field relationships, age and petrography

This group of high-Mg magmatic rocks forms an intrusion known as the Cagacaroon Syenogranite (Fig. 1), comprising a mesocratic K-feldspar porphyritic granite with amphibole as the major mafic phase (Fig. 3d). The pluton is a wedge-shaped intrusion, about 125 km^2 in size, and dated at 2747 ± 3 Ma (GA 99969142, Fletcher and McNaughton, 2002). It belongs to the Annean Supersuite of Van Kranendonk et al. (2013), and is contemporaneous with the transitional TTGs of the adjacent Yalgoo dome. It contains ubiquitous, elongate enclaves rich in amphibole (Fig. 3d) and its field appearance is similar to plutons of the Cullculli Suite described by Ivanic et al. (2012).

Primary magmatic textures are overprinted by a solid-state foliation, parallel to the contact with the greenstones. Large, euhedral K-feldspar and rare plagioclase porphyroclasts are deformed and surrounded by oriented aggregates of large hornblende and smaller biotite, epidote, titanite and magnetite. Occasionally, large amphibole grains preserve relict cores of recrystallized clinopyroxene.

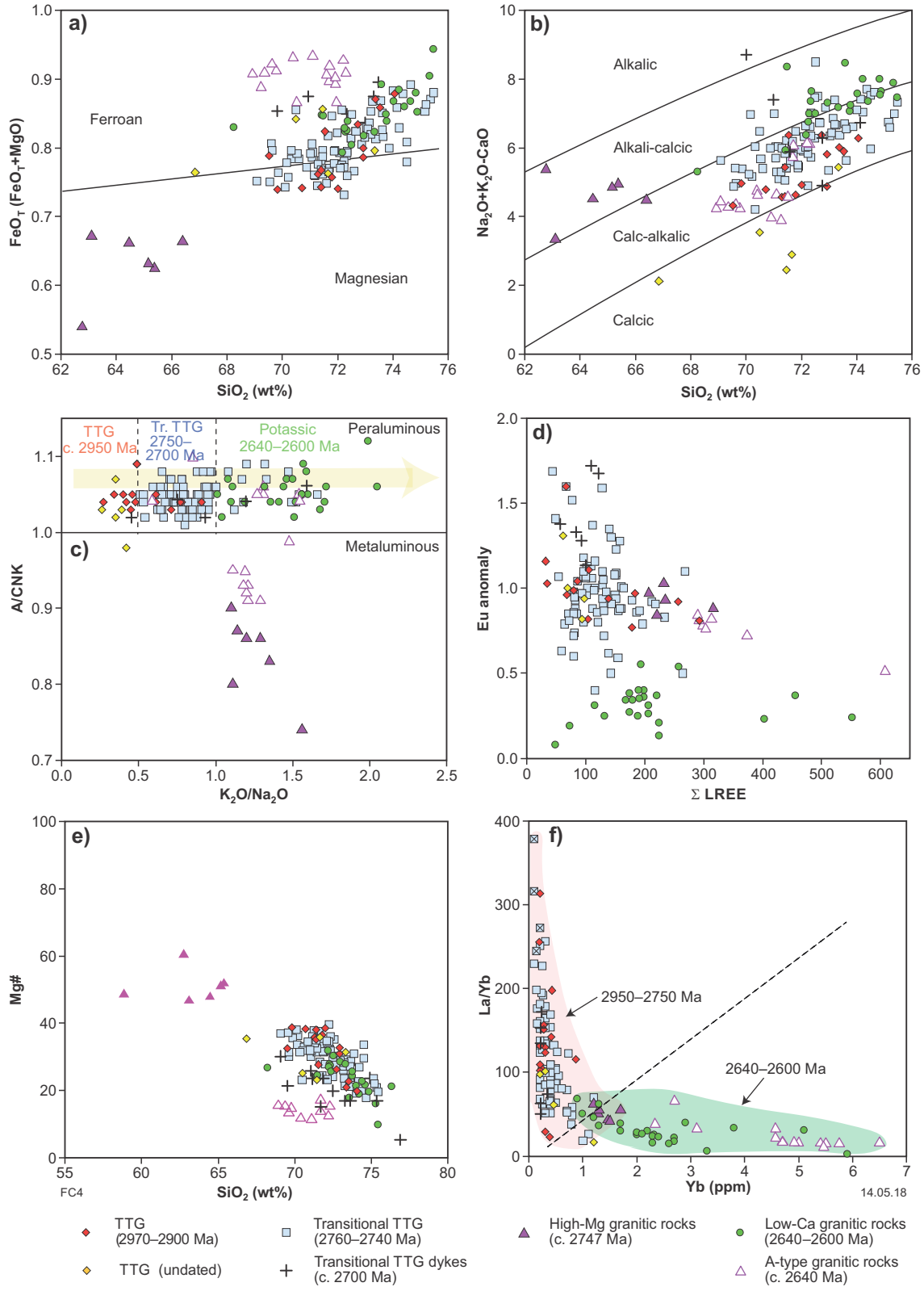

Figure 4. **Representative plots of the diverse late Archean granitic rocks from the Yalgoo dome: a) $FeO_T/(FeO_T + MgO)$ vs SiO_2 of major granite suites illustrating the difference between the A-type Damperwah pluton and high-Mg Cagacaroon Syenogranite; b) $Na_2O + K_2O–CaO$ vs SiO_2; most samples are calc-alkaline with the exception of the alkali-calcic samples of the Cagacaroon Syenogranite; c) aluminium saturation index (A/CNK) vs K_2O/Na_2O showing that TTG, transitional TTG, and low-Ca granitic rocks are slightly peraluminous and become increasingly rich in K_2O with time, whereas high-Mg and A-type granitic rocks are metaluminous with K_2O/Na_2O >1; d) Eu anomaly (Eu_N/Eu^* vs the sum of light rare earth elements (Σ LREE = La + Ce + Nd) where $Eu^* = \sqrt{Sm_N \cdot Gd_N}$ and concentrations are normalized to C1 chondrites (McDonough and Sun, 1995); e) Mg# ($Mg^{2+}/Mg^{2+} + Fe^{2+}$, with Fe_{Total} as Fe^{2+}) vs SiO_2; f) Yb vs La/Yb**

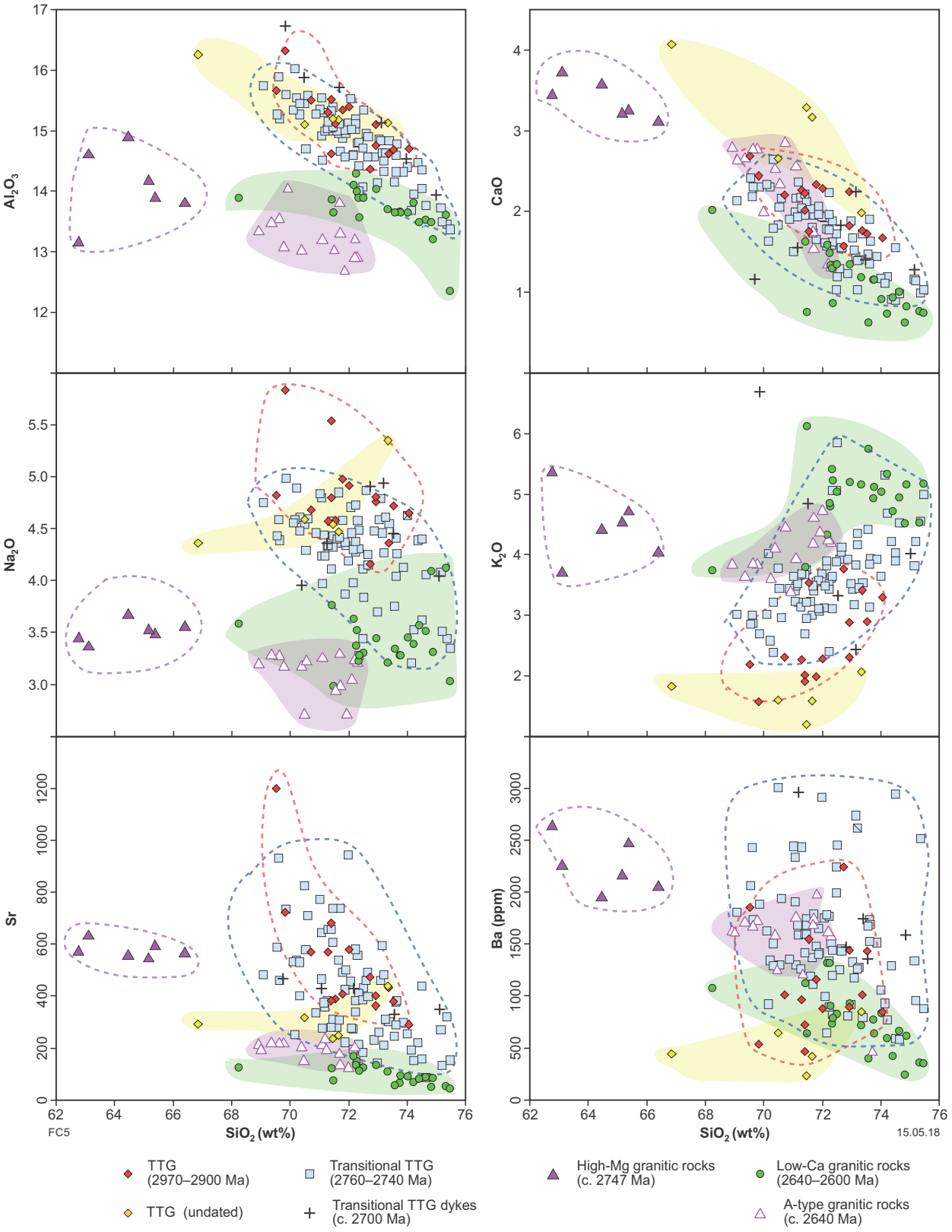

Figure 5. Representative major and trace elements vs SiO_2 for the five granitic rock groups in the Yalgoo dome

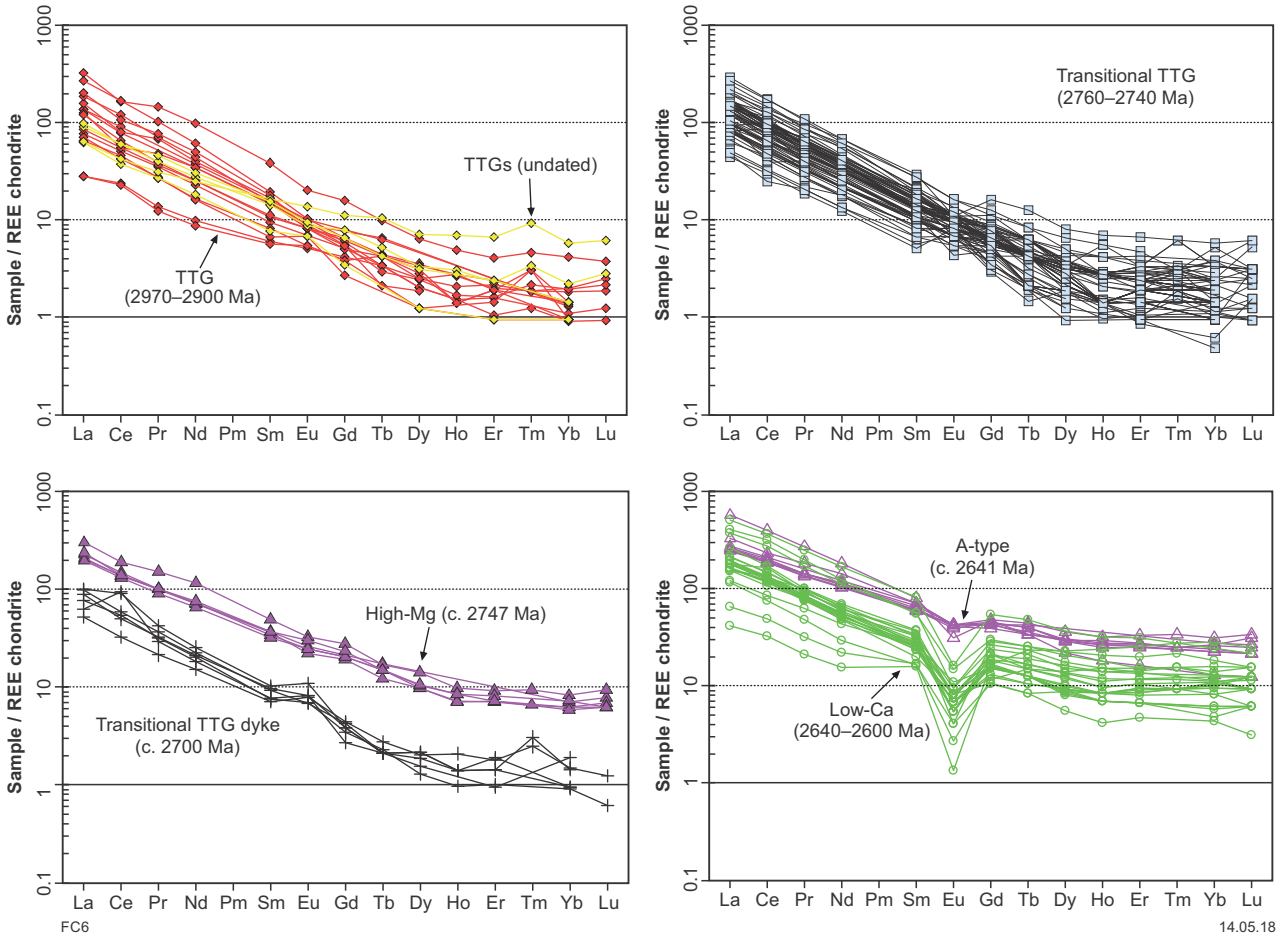

Figure 6. Chondrite-normalized REE diagrams (Boynton, 1984) for the main granitic rock groups

Geochemistry

Rocks of the Cagacaroon Syenogranite differ from other groups because of their magnesian (Fig. 4a), calc-alkalic to alkali-calcic (Fig. 4b) and metaluminous nature (Fig. 4c). The granodiorite displays high MgO (2.2 – 4.2 wt%), K_2O (3.7 – 5.4 wt%) and CaO (3.2 – 5.0 wt%) contents at low silica content (58.9 – 66.4 wt%) (Fig. 5). The most distinctive geochemical feature of these rocks is a trace element signature comparable to those of Archean sanukitoids (Martin et al., 2005, 2009; Heilimo et al., 2010; Laurent et al., 2014) and the geochemistry of the Cullculli Suite of the northern Murchison Domain (Ivanic et al., 2012). This includes strong LILE enrichments with Ba >2000 ppm, Sr = 565–768 ppm and Rb = 176–269 ppm (Fig. 5; Table 2) accompanied by moderate enrichment in mantle compatible elements, such as Cr (42–176 ppm), Ni (33–120 ppm) and V (67–127 ppm) (Table 2; Appendix). REE patterns are fractionated with La/Yb~50 (Fig. 4f) and moderate depletion in HREE (Fig. 6) ('spoon-shaped patterns' are comparable to Cullculli Suite rocks in the northern Murchison Domain, Fig. 4b, Ivanic et al., 2012). High field strength element (HFSE) contents are similar to TTGs and transitional TTGs, with low Zr (142–244 ppm) and Nb (6–11 ppm) concentrations, but La (62–93 ppm) and TiO_2 concentrations (0.5 – 0.9 wt%) are higher (Table 2).

A-type group: Damperwah and Seeligson Monzogranite

Field relationships, age and petrography

The Damperwah pluton and part of the Seeligson Monzogranite (Fig. 1) — both hornblende–biotite monzogranites — have outcrop areas of more than 220 km^2 and 270 km^2, respectively, south of the Yalgoo dome. The Damperwah pluton has been dated at 2641 ± 5 Ma (GSWA 83407, Wiedenbeck and Watkins, 1993). Like the slightly younger low-Ca granitic rocks (described below), the Damperwah and Seeligson plutons have subcircular, discordant outcrop shapes or map patterns that cut stratigraphic units and tectonic features associated with folding in the greenstones. Igneous textures lacking solid-state overprint suggest that the intrusion post-dated the peak of regional deformation and genesis of the Yalgoo dome. This monzogranite pluton is rich in hornblende diorite or pyroxene diorite and banded iron-formation enclaves (Fig. 3f), ranging in size from a few centimetres up to several metres. Mineral paragenesis is defined by aggregates of Fe-rich hornblende, biotite, quartz and ilmenite surrounded by plagioclase, quartz and rare K-feldspar porphyroclasts. Minor amounts of fayalitic olivine, clinopyroxene, apatite and zircon are common, but do not occur in all samples (Wiedenbeck and Watkins, 1993).

Geochemistry

This pluton is a felsic (68.9 – 72.3 wt% SiO_2), calc-alkalic, ferroan and metaluminous to peraluminous monzogranite (Fig. 4a–c), comparable to A-type granitic rocks worldwide (Eby, 1992; Frost and Frost, 2011). Like low-Ca granitic rocks, it shows low Al_2O_3 (12.9 – 13.8 wt%) and Na_2O (2.9 – 3.2 wt%), but K_2O (3.8 – 4.6 wt%) and CaO (1.3 – 2.8 wt%) contents are similar to those of transitional TTGs (Fig. 4), resulting in K_2O/Na_2O >1 (Fig. 4c). For a given silica content, it is significantly enriched in HFSE with the highest Zr (265–521 ppm), Hf (12–13 ppm), Y (36–68 ppm) and TiO_2 (0.3 – 0.6 wt%) concentration among all granite groups studied here. HREE contents are very high (Fig. 6) and define a 'seagull-shaped' REE pattern with La/Yb~10 (Fig. 4f) and a moderate negative Eu anomaly (Eu*/Eu~0.8 – 1.0; Fig. 4d). The relative behaviour of the LILE differs from that in the other granitic types in that Ba, Rb and Pb are enriched, as in the other granitic groups, but Sr is strongly depleted and shows values comparable only to those of low-Ca granitic rocks (Fig. 5; Table 2). Many of the chemical features of the Damperwah and Seeligson plutons are also shared with the contemporaneous low-Ca group. The Damperwah A-type pluton is more enriched in CaO and depleted in K_2O than the low-Ca group, but has a similar Sr-Al_2O_3 depletion (Fig. 4) and high HREE content (Fig. 6), which indicate generation at moderate crustal pressures <10 kbar, outside the stability field of garnet.

Low-Ca granitic rocks

Field relationships, age and petrography

Low-Ca granitic rocks form post-tectonic intrusions with subcircular map patterns, which truncate older rocks in the Yalgoo dome and surrounding greenstones (Fig. 1). Contacts with country rocks are sharp and weakly deformed. They are coarse-grained (Fig. 3e), equigranular leucogranites with K-feldspar-rich domains surrounded by quartz, plagioclase, biotite with minor chlorite, and muscovite. They are dated at 2626 ± 6 Ma (GSWA 207630, Wingate et al., 2014) and 2602 ± 14 Ma (GSWA 83551, Wiedenbeck and Watkins, 1993) and are compositionally related to the contemporaneous post-tectonic granitic rocks of the 2640–2600 Ma Bald Rock Supersuite (Van Kranendonk et al., 2013) reported throughout the Yilgarn Craton (Champion and Sheraton, 1997). Because of this similarity, we interpret the age of these granitic rocks to be within the range of the Bald Rock Supersuite (2640–2600 Ma).

Geochemistry

Low-Ca granitic rocks are calc-alkaline and peraluminous rocks (Fig. 4b,c), and are the most potassic of the five groups described here (K_2O/Na_2O >1; Fig. 4c). For a given SiO_2 content (71.0 – 75.0 wt%) they show lower Al_2O_3 (11.08 – 14.28 wt%), CaO (<2.0 wt%), Na_2O (<4.1 wt%), and higher K_2O (3.7 – 6.1 wt%) contents than the TTGs and transitional TTGs (Fig. 5). Compared to transitional TTGs, HFSE concentrations are high (Nb = 5–42 ppm, La = 37–156 ppm; Th = 14–84 ppm; U = 4–93 ppm, Y = 10–81 ppm) despite highly variable Zr (81–524 ppm) and Hf (3.3 – 9.5 ppm) concentrations. Concentrations of Ba (110–1300 ppm) and Sr (22–166 ppm) are lower, but those of Rb (172–453 ppm), Pb (22–107 ppm) and Li (6–57 ppm) are higher (Table 2). Chondrite-normalized REE in Figure 6 show a seagull-like pattern (cf. Fig. 4e,f, Walganna and Wogala Suites, Ivanic et al., 2012), defined by relatively high HREE content (Yb = 1–6 ppm; Table 2), La/Yb <25 (Fig. 4f) and a marked negative Eu anomaly (Eu*/Eu <0.5; Fig. 4d).

Discussion

In the Yalgoo dome, and its most immediate surroundings, we identified five granitic groups that collectively indicate >300 Ma of magmatic evolution, which can be divided into four stages based on the distinctive age, geochemical signature and structural location of each granite group within the dome (Fig. 2). TTGs define Stage 1 (2970–2900 Ma), high-Mg granitic rocks and transitional TTGs in Stage 2 (2760–2740 Ma), transitional TTG dykes in Stage 3 (c. 2700 Ma) and A-type and low-Ca rocks in Stage 4 (2760–2740 Ma) (Fig. 7). We first describe each of the four stages before dividing them into three major phases based on correlation with major episodes of mantle-derived magmatism that formed the greenstones (Fig. 7).

Stage 1: TTG magmatism (2970–2900 Ma)

Geochemical modelling by Moyen (2011) showed that TTGs can be divided into three groups, based on different melting pressures in the source. At low pressure (12–15 kbar), mafic rocks exhibit a garnet-poor, plagioclase-rich mineral paragenesis (Moyen and Martin, 2012), and melts derived from this assemblage are enriched in HREE, but depleted in elements compatible in plagioclase such as Sr, Na and Al. These felsic melts produce rocks equivalent to the low-Al TTG of Barker and Arth (1976). By contrast, at high pressures (P >20 kbar), melting of mafic rocks produces felsic melts with high Na, Al and Sr, but low HREE, suggesting a garnet-rich, but plagioclase-free (i.e. eclogitic) residue. Between these two end-members is a third group that forms between 15 and 20 kbar and displays an intermediate geochemical signature, reflecting a source with abundant garnet and amphibole, but minor plagioclase.

Phase equilibrium modelling of an enriched Archean tholeiite by Palin et al. (2016) indicates that TTG magmas can develop at ~800–950°C and ~10–18 kbar. Moreover, these authors contend that the protolith is most fertile (15–35% melting) when crossing the wet solidus at P ~11–12 kbar and that the three groups introduced by Moyen (2011) could form from the same source, at various depths and temperatures during the same tectono-metamorphic episode. Similarly, the melting experiments of Qian and Hermann (2013) and Zhang et al. (2013) demonstrated that low to intermediate pressure TTGs can be generated by anatexis of hydrous mafic rocks at 800–950°C and 10–12 kbar. In addition, Johnson et al. (2017) showed that low-Mg basalts, such as the Coucal Formation in the Pilbara Craton, have the potential to generate TTG melts at pressures as low as 7 kbar.

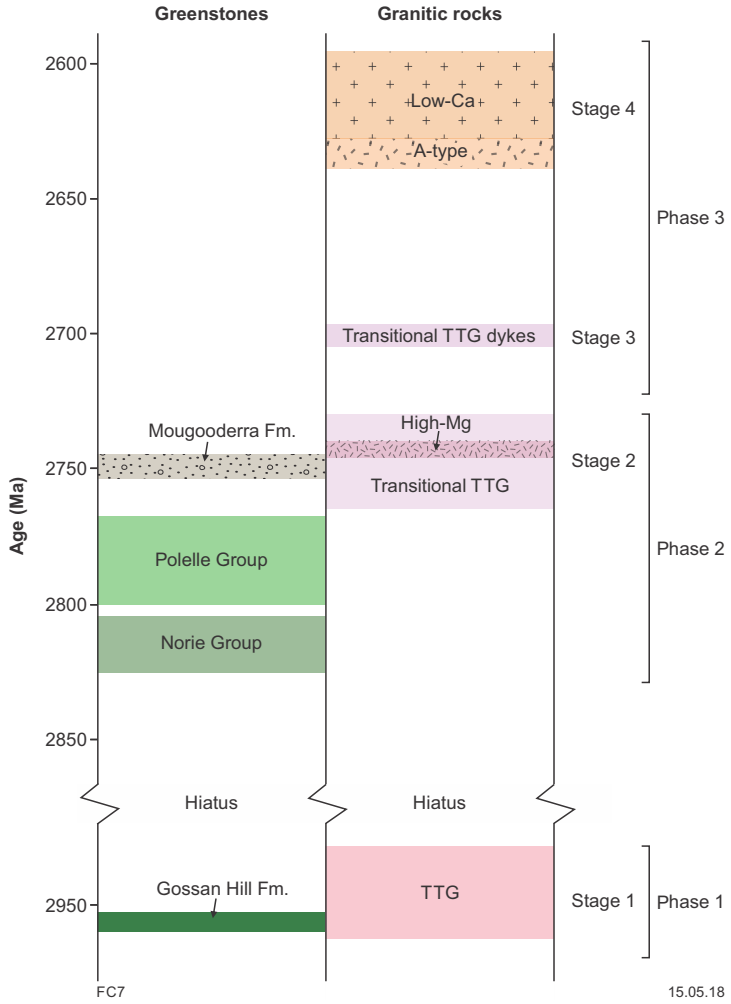

Figure 7. **Temporal relationships between greenstones and granitic rocks in the Yalgoo dome and the four stages of felsic magmatism that constitute three phases of mantle-derived magmatism (i.e. greenstones) followed by crustal reworking (i.e. granitic rocks). Phase 3 greenstones are absent in the Yalgoo dome area, but have been reported in the northeastern Murchison Domain (see legend Fig. 1) (Ivanic et al., 2012; Van Kranendonk et al., 2013)**

The difficulty with interpreting TTGs is that melting within this range of conditions might occur in more than one geodynamic setting (Arth and Hanson, 1975; Condie, 1981; Martin, 1986). Indeed, in the last three decades, the ideal geodynamic setting for the origin of TTGs has been intensely debated between proponents of subduction zones (Defant and Drummond, 1990; Moyen and Martin, 2012) and those who favour melting at the base of oceanic plateaux or tectonically overthickened crust (Collins et al., 1998; Smithies et al., 2009; Van Kranendonk et al., 2015). These are just some of the numerous models proposed in the attempt to reconcile the formation of Archean TTGs to a tectonic setting. This remains elusive because several mechanisms and settings have the potential to generate TTG-like magmas (e.g. Sizova et al., 2015).

Stage 2: high-Mg granitic rocks and transitional TTGs (2760–2740 Ma)

Following Stage 1, felsic magmatism resumed in the Yalgoo dome at c. 2760 Ma. Granitic rocks are dominated by 2760–2740 Ma transitional TTGs that were accompanied by intrusion at c. 2747 Ma of the high-Mg Cagacaroon Syenogranite in the greenstone cover (Fig. 1). They are grouped together not only because they occurred at the same time but also because their origins could be related. In this section, we briefly outline the mainstream genetic model for the genesis of high-Mg granitic rocks and transitional TTGs, then we propose an integrated model to explain their coeval occurrence in the Yalgoo dome.

Origin of high-Mg granitic rocks: Cagacaroon Syenogranite

High-Mg granitic rocks enriched in Cr, Ni and LILE are viewed by some authors as sanukitoids; hence, they are often related to a source component derived from subduction-metasomatized lithosphere (Shirey and Hanson, 1984; Martin et al., 2005, 2009; Heilimo et al., 2010). In a convergent setting, sanukitoids can form by two distinct processes, depending on the degree of interaction between slab-derived melts and mantle wedge peridotite. The first is a one-step process, in which slab-derived melts incorporate or digest variable amounts of peridotite before crustal emplacement (Rapp et al., 1999, 2010). The second is a two-step process, in which slab-derived melts react completely with mantle peridotite during ascent, and crystallize in the mantle wedge to create an enriched mantle, including variable proportions of phlogopite and pargasite (Martin et al., 2005, 2009). A subsequent thermal anomaly can destabilize this metasomatized mantle and generate sanukitoids up to several hundred million years after the emplacement of the TTG melt (Stern and Hanson, 1991; Rapp et al., 1999, 2010; Laurent et al., 2014).

Given that the only modern geodynamic environment capable of supplying sufficient volumes of hydrous and LILE-enriched metasomatic agents to the upper mantle is a subduction zone, many authors contend that similar processes would have characterized the Archean (Heilimo et al., 2010; Farina et al., 2015). However, granitic rocks with a sanukitoid-like signature are also reported in other geological contexts. For example, intracontinental high-Mg granitic rocks in the North China Block are viewed as having formed by partial melting of mafic rocks during regional lower crust delamination in the Cretaceous (Gao et al., 2009). In this case, delaminating mafic lower crust has the potential to produce melts with TTG-like compositions that might interact with peridotites before intruding the crust, forming high-Mg (i.e. sanukitoids) intrusions. Another example is the occurrence of K-rich granitic rocks enriched in Mg, Cr and Ni along the Red River – Ailao and Shan–Batang–Lijiang faults in eastern Tibet (Campbell et al., 2014). At various points along this 1500 km long transpressional lineament, continental crust was down-thrusted into the upper mantle, where it melted and interacted with overlying mantle rocks (see fig. 7 in Campbell et al., 2014). In essence, high-Mg granitic rocks formed along crustal-scale structures that tapped a previously enriched mantle.

Origin of transitional TTGs

In many Archean terranes, granitic rocks with transitional TTG compositions are viewed as hybrids, formed by mixing and mingling of different magmas. For instance, the hybrid granitic rocks in the Limpopo Belt (Laurent et al., 2014) display multiple evidence for a mixing origin, such as rapakivi-textured feldspars, quartz ocelli, magma mingling and a bulk chemistry inconsistent with melting of a single source. Likewise, the geochemical modelling of Almeida et al. (2010) shows that mixing between fractionated high-Mg granitic rocks (i.e. sanukitoids) and trondhjemitic melts derived from partial melting of mafic metavolcanic rocks can account for the chemical signatures of transitional TTGs in the Amazonia Craton.

The mixing hypothesis has been successfully applied in the Limpopo Belt in South Africa by Laurent et al. (2014) to explain the contemporaneous appearance of high-Mg (i.e. sanukitoids) and transitional TTGs but it may not be relevant to the Yalgoo dome. In contrast to the Limpopo Belt, transitional TTGs in the Yalgoo dome lack textural evidence for magma mixing and mingling. Also, their chemical compositions are different: transitional TTGs in the Yalgoo dome are less potassic, lack silica-poor members (SiO_2 <70 wt%) and are consistently more enriched in Ba (Fig. 8). If mixing between TTG melts and high-Mg magmas occurred in the Yalgoo dome, the hybrids would have been homogenized and fully equilibrated. Alternatively, transitional TTGs might have formed by entirely different processes.

Following Champion and Smithies (2007), we suggest that the geochemical signatures of transitional TTGs in the Yalgoo dome reflect their source. High LILE, Th and U concentrations are characteristic of Archean granitic rocks comprising material from older felsic crust (Moyen, 2011). However, the older 2970–2900 Ma TTGs that crop out at the present erosion surface are not suitable sources, because they have similar bulk compositions (70–75 wt% SiO_2), but lower K_2O content, than transitional TTGs. Given that the 2760–2740 Ma transitional TTGs have the same bulk compositions and REE depletions as most Archean TTGs, but are more enriched in LILE and radiogenic elements, we propose that they formed from an unexposed basaltic source in the deep crust, which was more enriched and evolved than the average basaltic source for TTGs. Alternatively, felsic volcanic and sedimentary rocks interbedded with basalts could generate enriched TTG melts (Champion and Smithies, 2007).

Lithospheric reworking

The contemporaneity of high-Mg felsic magmas and transitional TTGs in the Yalgoo dome can be interpreted as in situ melting of a lithospheric column comprising a metasomatized mantle and an overlying felsic–mafic crust. A three-step model is suggested. The first step involved metasomatization of the subcontinental lithospheric mantle (SCLM). The second step involved mantle melting that culminated in eruption of the Norie Group (2825–2805 Ma) and the ~8-km thick Polelle Group (2800–2760 Ma; Ivanic et al., 2012; Van Kranendonk et al., 2013; Ivanic et al., 2015). The rise in temperature from mafic underplating, thermal blanketing from the erupted greenstones (Rey et al., 2003) and radioactive decay in buried felsic rocks caused partial melting of both crust and metasomatized SCLM, generating high-Mg melts and transitional TTGs (Fig. 9). The third step involved high-Mg magmas that ascended to the base of the crust, where some ponded and triggered further melting of enriched basalts in the lower crust to develop more transitional TTGs; others, perhaps more fractionated and buoyant magmas, rose with little interaction with the lower crust to form high-Mg intrusions (Fig. 9). A variant of this model was proposed by Ivanic et al. (2012), in which high-Mg granitic rocks were interpreted to have formed by mixing of mafic and felsic magmas rather than partial melting of a metasomatized mantle.

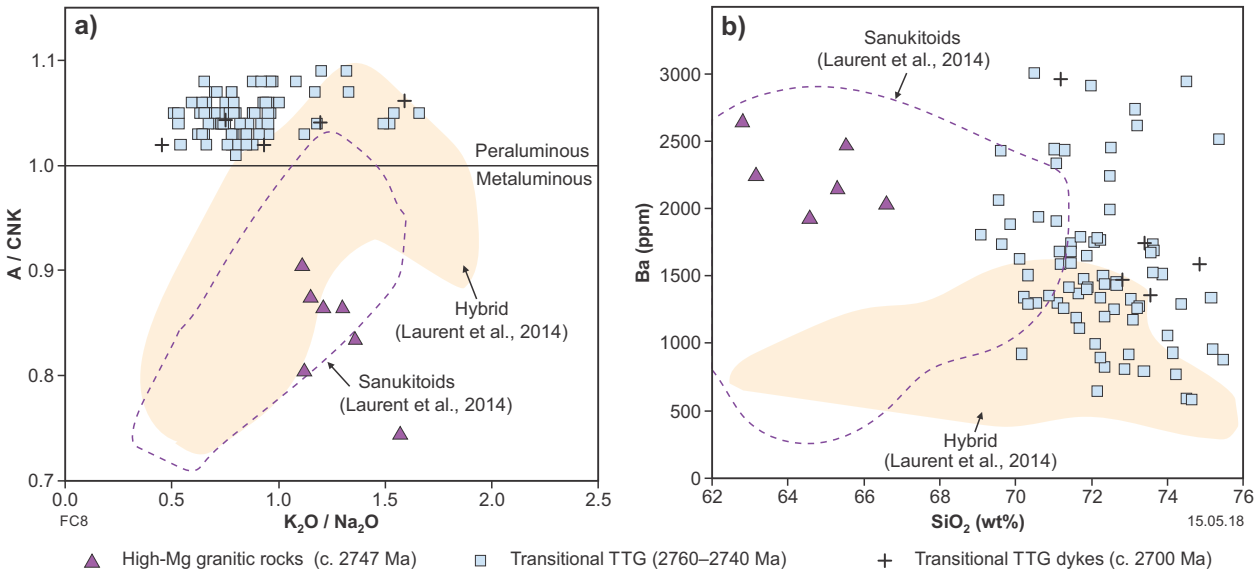

Figure 8. **a) Aluminium saturation index (A/CNK) vs K_2O/Na_2O; b) Ba vs SiO_2 for high-Mg granitic rock and transitional TTGs of the Yalgoo dome, compared with sanukitoids and hybrid granitic rocks (derived from mixing of sanukitoids and crustal melts) from Laurent et al. (2014)**

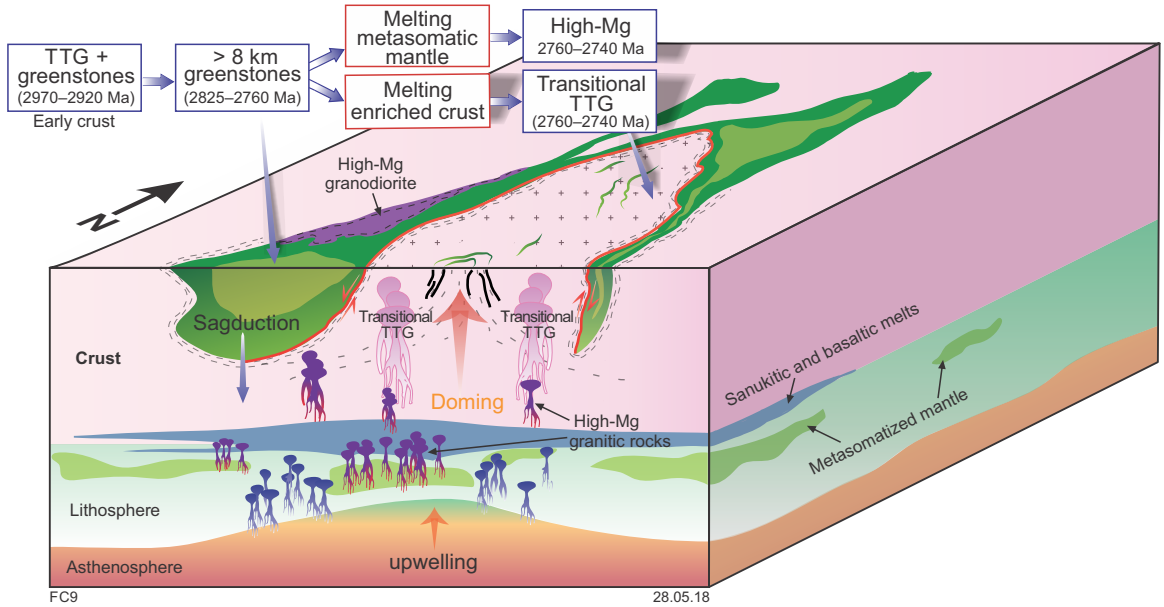

Figure 9. **Schematic diagram showing the scenario at 2760–2740 Ma (Stage 2) in which coeval transitional TTGs and high-Mg granitic rocks are formed during the main dome-forming event**

Stage 3: transitional TTG dykes (c. 2700 Ma)

In the Murchison Domain, Phase 2 of crustal formation was initiated by Stage 3 of mantle-derived melts, including komatiitic basalts of the 2735–2710 Ma Yalgowra Suite and c. 2720 Ma Glen Group (Ivanic et al., 2012). This renewed mantle-derived magmatism induced a second and more pronounced phase of crustal reworking with emplacement of voluminous felsic plutons with mainly TTG compositions during the 2730–2660 Ma interval. These TTGs are contemporaneous with an anastomosing craton-scale network of Neoarchean transpressive shear zones that accommodated regional east–west shortening during Neoarchean (<2730 Ma) orogenic events (Zibra et al., 2017a).

Stage 3 is recorded by north-trending shear zones and the emplacement of granitic dykes (c. 2700 Ma; Fig. 3b), contemporaneous with emplacement of the 2710–2695 Ma Lakeside pluton, a voluminous intrusion adjacent to the Yalgoo dome (Fig. 1; Zibra et al., 2014a). We conclude that the same tectono-magmatic episode caused the intrusion of a swarm of granitic dykes in the Yalgoo dome and the Lakeside pluton. However, granitic rocks in the Lakeside pluton are mainly TTGs (Zibra et al., 2014a), whereas the granitic dykes are comparable to the more abundant 2760–2740 Ma transitional TTGs (Figs 4, 6; Stage 2). This suggests that they might have been derived from reactivation of the same enriched source that generated the 2760–2740 Ma transitional TTGs (Fig. 10).

Stage 4: post-tectonic granites (2640–2600 Ma); A-type and low-Ca granitic rocks

Transitional TTG dykes emplaced during Stage 3 were followed by the emplacement of two groups of post-tectonic, undeformed K-rich granitic rocks between 2640 and 2600 Ma: the A-type intrusions in the Damperwah and Seeligson plutons (Fig. 1) and numerous low-Ca plutons of the Bald Rock Supersuite (Van Kranendonk et al., 2013).

Origin of A-type granitic rocks

There are many controversies regarding the origin of A-type granitic rocks, because they appear to be attributable to fractionation of mantle-derived mafic magmas, to high-temperature, dry partial melting of quartzofeldspathic rocks in the crust, or to mixing processes (Eby, 1992; Skjerlie and Johnston, 1992). Under some conditions, fractionation of mantle-derived mafic magma generates melts with alkaline compositions (King et al., 1997; Frost and Frost, 2011). The metaluminous to weakly peraluminous nature of the calc-alkaline Damperwah pluton (Fig. 4c) argues against this origin. The high SiO_2 (>69.0 wt%; Fig. 5) content combined with high Ba concentrations (Fig. 4; Table 2) implies that an origin by fractional crystallization of mantle-derived magmas is unlikely, and suggests instead that they might have formed by low-pressure, high-temperature melting of residual rocks in the crust or by mixing of basaltic and granitic magmas (Whalen et al., 1987; Frost and Frost, 2011).

The chemical compositions of the Damperwah and Seeligson plutons are analogous to Paleoproterozoic A-type granitic rocks exposed along the margin of the Archean North China Craton (Deng et al., 2016) and in Carajás, Brazil (Dall'Agnol and de Oliveira, 2007). The main petrogenetic models proposed for these terranes advocate low-pressure, high-temperature partial melting of Neoarchean calc-alkaline rocks at low (Deng et al., 2016) or high oxygen fugacity (Dall'Agnol and de Oliveira, 2007). We propose that the A-type intrusions in the Yalgoo dome formed in a similar way. The pervasive presence of ilmenite and Fe-rich amphibole in the Damperwah pluton, as observed also in Paleoproterozoic A-type granitic rocks in China (Deng et al., 2016), indicates low oxygen fugacity (Anderson and Smith, 1995).

Notwithstanding questions about the petrogenesis of A-type granitic rocks, it is widely accepted that they form in extensional regimes, either post-orogenic or anorogenic (Whalen et al., 1987; Frost and Frost, 2011). These two settings can be differentiated chemically according to the diagrams of Eby (1992) (Fig. 11). Eby's A_1 group represents alkaline granitic rocks formed by fractional crystallization of basalts in an anorogenic setting. His A_2 group comprises post-orogenic, calc-alkaline granitic rocks, such as post-tectonic A-type granitic rocks typical of most Proterozoic terranes (Frost et al., 1999; Dall'Agnol and de Oliveira, 2007; Duchesne et al., 2010; Deng et al., 2016). The Damperwah pluton presented here corresponds to the A_2 group because of its elevated Rb/Nb and Y/Nb (Fig. 11) and, as suggested by Eby (1992), it could be generated from melting of quartzofeldspathic crust or, less likely, by fractionation of underplated mafic magmas that have undergone continent–continent collision or island-arc magmatism.

Origin of low-Ca granitic rocks

Most authors consider low-Ca granitic rocks to be derived from low-degree partial melting of felsic rocks (TTGs, felsic volcanic rocks) at shallow crustal depths (Whalen et al., 2004; Frost et al., 2006; Almeida et al., 2013; Farina et al., 2015). Their geochemistry suggests that plagioclase fractionation or plagioclase retention in the source played a key role, resulting in melts depleted in Sr, Al, Na and Ca with marked negative Eu anomalies (Dey et al., 2012; Farina et al., 2015).

Lower crust delamination

The sudden change in the nature of magmatism from TTGs to A-type and low-Ca across the Yilgarn Craton needs to be explained by wide regional changes. Ivanic et al. (2012) proposed a delamination model to link the change in chemical composition of 2640–2600 Ma granitic rocks to a post-tectonic environment. Following the end of Neoarchean orogenic events, removal of lower crust by delamination would result in asthenospheric upwelling that could have heated the crust sufficiently. In these models, A-type and low-Ca granitic rocks would form by high-temperature dehydration melting of quartzofeldspathic rocks in the upper crust (Fig. 12; Ivanic et al., 2012).

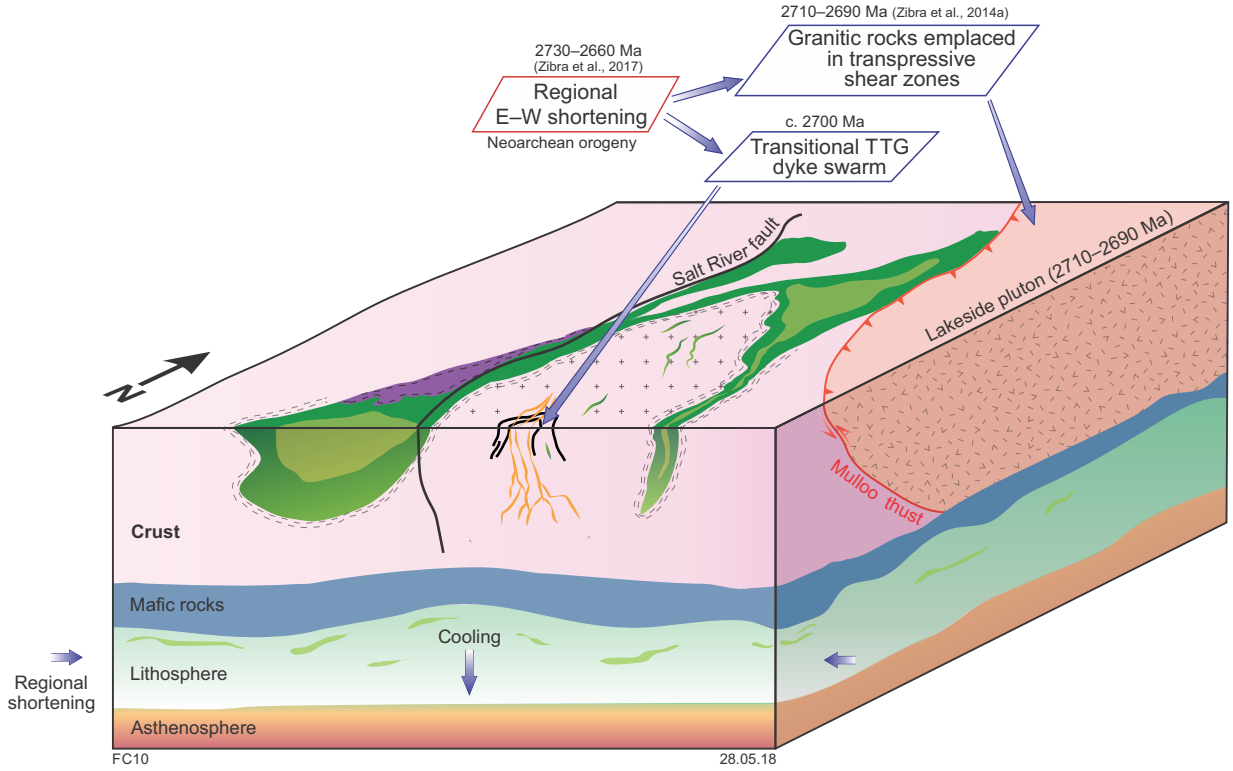

Figure 10. Schematic diagram showing the effects of Neoarchean orogenic events at 2730–2660 Ma (Stage 3) orogeny in the Yalgoo dome. East–west regional shortening caused the emplacement of the voluminous 2710–2690 Ma Lakeside pluton and transitional TTG dykes in the Kynea Tonalite in the core of the dome

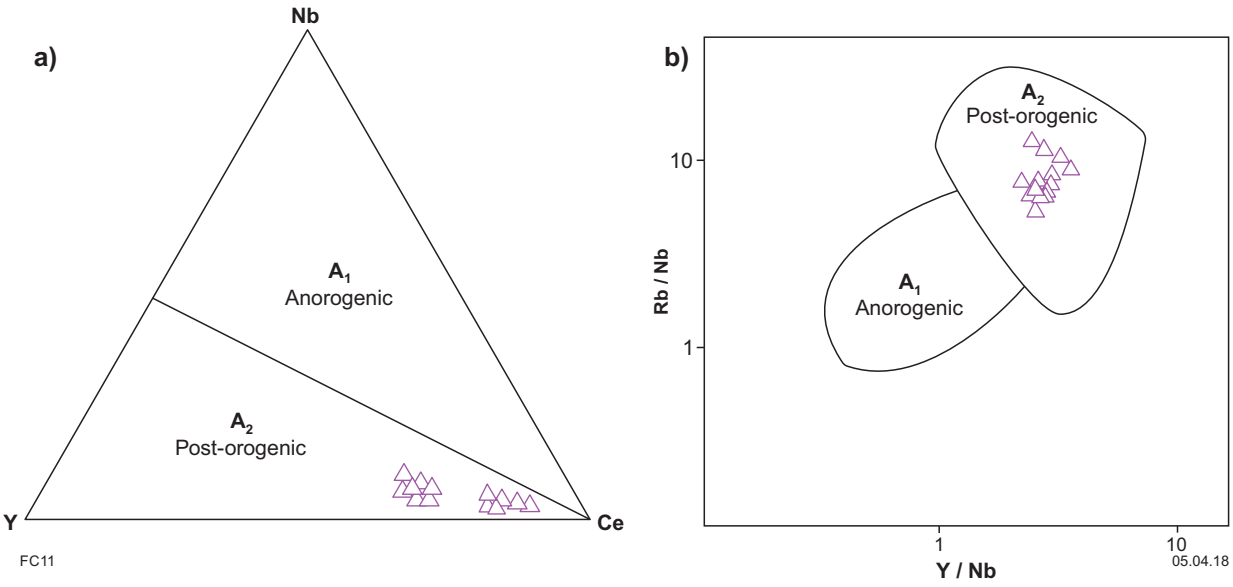

Figure 11. Discrimination diagrams for A-type granitic rocks of the Damperwah pluton (after Eby, 1992): a) A_1 corresponds to the field of alkaline A-type granitic rocks formed in an anorogenic setting by fractional crystallization of basalts; b) A_2 field corresponds to calk-alkaline A-type granitic rocks typical in a post-orogenic environment

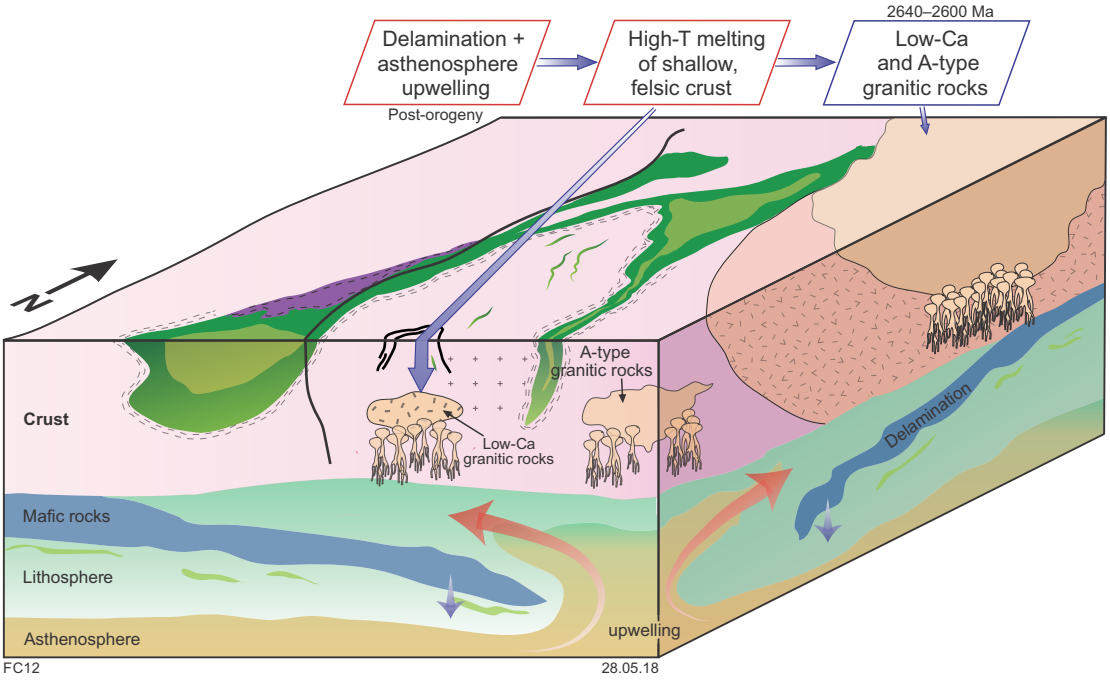

Figure 12. Schematic diagram showing post-orogenic events (2640–2600 Ma, Stage 4) in the Yalgoo dome. After the end of Neoarchean orogenic events (Stage 3), regional delamination could have resulted in asthenospheric return flow that would have heated the crust and allowed high-temperature dehydration melting of more evolved rocks in upper levels of the crust, forming both A-type and low-Ca granitic rocks

In the Yalgoo region, the geochemistry of the A-type Damperwah and Seeligson plutons is consistent with emplacement in a post-orogenic extensional environment, as suggested by Champion and Sheraton (1997) and Cassidy et al. (2002) for identical granitic rocks (their high-HFSE granitic rocks) in the Eastern Goldfields Superterrane (Fig. 1). In addition, because A-type and low-Ca plutons show comparable Sr-Al_2O_3 depletion (Fig. 4) and high HREE content (Fig. 5), it is probable that they formed in a similar tectono-magmatic environment, but from slightly different sources and at different crustal levels.

Crustal reworking and implications for incremental formation of Archean continental crust

The four stages of granitic activity, at 2970–2900 Ma, 2760–2740 Ma, c. 2700 Ma and 2640–2600 Ma, were linked to three distinct phases of enhanced mantle activity (Figs 7, 13). These episodes of mantle-derived mafic–ultramafic magmatism resulted in repeated crustal reworking, resulting in the intrusion of granitic rocks. Phase 1 was marked by the coeval formation of Stage 1 TTGs and greenstones of the 2963–2958 Ma Gossan Hill Formation (Fig. 7). This earliest reworking episode involved an older mafic crust, the partial melting of which generated the TTG magmas at 2970–2900 Ma. Following a magmatic hiatus of more than 100 Ma, Phase 2 began with eruption of the 2825–2805 Ma Norie Group and voluminous 2800–2760 Ma Polelle Group (Ivanic et al., 2012; Van Kranendonk et al., 2013; Ivanic et al., 2015) and culminated with the diapiric emplacement of Stage 2 granitic rocks (Fig. 7). The time lag between greenstone deposition and granitic intrusion may have simply reflected the time necessary to heat the lithosphere. This thermal insulation resulted in reheating and remobilization of a mafic–felsic crust, resulting in intrusion of transitional TTGs, and metasomatization of its underlying mantle resulted in the intrusion of high-Mg granitic rocks. This short-lived episode (c. 20 Ma) of crustal reworking was dominated by buoyant forces of plutonic and migmatitic bodies resulting in the vertical rearrangement of the crust in a negligible regional stress field.

The onset of Phase 3 (Fig. 7) is associated with a new stage of mantle-derived melts, with komatiitic basalts such as those of the 2735–2710 Ma Yalgowra Suite and c. 2720 Ma Glen Group, which outcrop only in the northern Murchison Domain (Ivanic et al., 2012). Although crustal reworking was dominant in the northwestern Murchison Domain and in the Southern Cross Domain, Phase 3 in the Yalgoo dome was initiated in an orogenic setting of east–west shortening that resulted in the emplacement of Stage 3 transitional TTG dykes during Neoarchean (2730–2640 Ma) orogenic events (Zibra et al., 2017a). This phase was followed by post-orogenic A-type and voluminous low-Ca granitic rocks of Stage 4 (Figs 7, 13). These crustal reworking events involved increasingly larger amounts of previously formed felsic rocks and give rise to K-rich granitic intrusions. In particular, the final development (Stage 4) of crust in the Yalgoo dome occurred during the intrusion of A-type and low-Ca granitic rocks, granitic rocks generated by high-temperature, low-pressure partial melting of quartzofeldspathic sources.

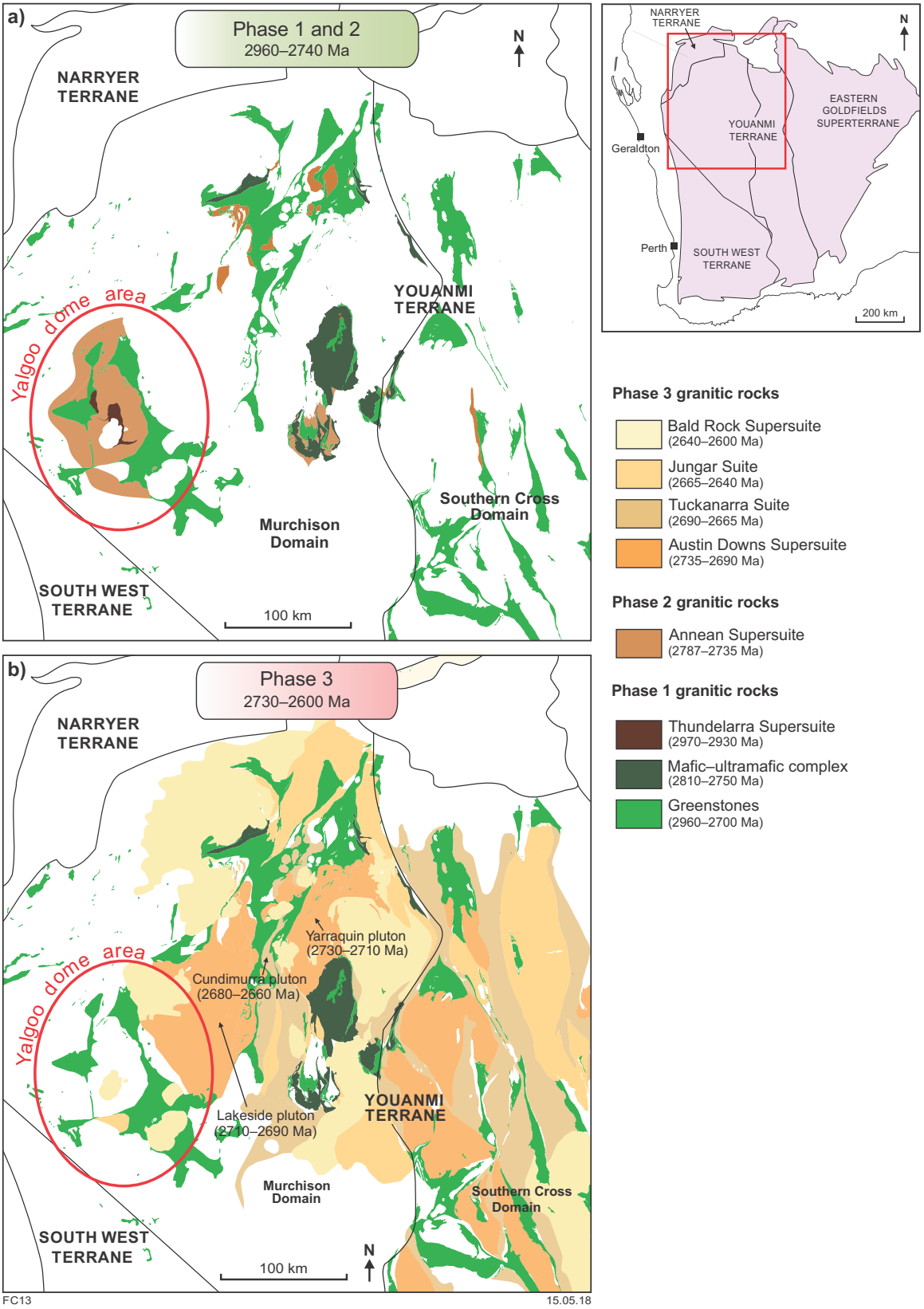

Figure 13. **Distribution of granitic rocks related to the three phases of crustal reworking in the Youanmi Terrane (Ivanic et al., 2012; Van Kranendonk et al., 2013): a) Phase 1 and Phase 2 granitic rocks comprise, respectively, the Thundelarra Supergroup (2970–2930 Ma) and Annean Supergroup (2787–2735 Ma). These units are well preserved only in the westernmost part of the terrane, where the Yalgoo dome is exposed; b) most of the terrane is intruded by Phase 3 granitic rocks, mainly intruded in a network of anastomosing shear zones coeval with emplacement of syntectonic granitic rocks of the Austin Downs Supersuite (2735–2690 Ma) and Tuckanarra Suite (2690–2665 Ma). Note the location of the Yarraquin pluton (2730–2710 Ma; Zibra et al., 2017a), Lakeside pluton (2710–2690 Ma; Zibra et al., 2014a) and Cundimurra pluton (2680–2660 Ma; Zibra et al., 2014b). Phase 3 was dominated by east–west compression followed by emplacement of numerous post-tectonic plutons of the Bald Rock Supersuite (2640–2600 Ma)**

These peak ages are corroborated by recent Lu–Hf isotope data on zircons from mainly granitic rocks in the northwest Murchison Domain (Ivanic et al., 2012). Early 2970–2920 Ma granitic rocks display ε_{Hf} between –4 and +2 and were interpreted as juvenile input into a Mesoarchean to Paleoarchean crust (Ivanic et al., 2012). Phase 2 of juvenile magmatism at 2825–2760 Ma shows rocks with ε_{Hf} from 0 to +3 derived from a c. 3040 Ma source. A sudden change in the melting source occurred at 2760–2730 Ma, indicated by felsic volcanic rocks of the Greensleeves Formation and granitic rocks of the Annean Supersuite, which show a wide array of ε_{Hf}, from –10 to 0, interpreted to reflect incorporation of a 3.7 – 3.0 Ga component in the source. The ε_{Hf} for c. 2720 and 2640 Ma granitic rocks indicates reactivation of a c. 3040 Ma source. The 2640–2600 Ma Bald Rock Suite is characterized by ε_{Hf} between –12 and –4, interpreted to indicate melting of a source as old as 3.8 Ga or mixing with a more juvenile component between 3.0 and 2.7 Ga.

The >300 Ma magmatic evolution of the Yalgoo dome has several ramifications for the formation and evolution of crust at the end of the Archean. Three processes must take place to develop a felsic continental crust: 1) sequential phases of mantle-derived, mafic–ultramafic magmatism accompanied by crustal reworking, culminating in the intrusion of granitic rocks; 2) the source of granitic rocks evolves from basaltic to felsic; and 3) the anatectic recycling zone becomes progressively shallower with time (cf. post-2750 Ma rocks in Ivanic et al., 2012). Our data support the in situ incremental growth of continental crust, but in a stepwise manner linked to major stages of crustal reworking at 2970–2900 Ma, 2760–2740 Ma, c. 2700 Ma and 2640–2600 Ma. Intermittent episodes of enhanced mantle activity added juvenile material and reheated the entire crust, causing reworking on a scale and style exclusive to the Archean.

Conclusion

The different granitic rocks throughout all late Archean cratons are comparable both in terms of their chemistry and relative timing, and can be separated into five groups: TTG, transitional TTG, high-Mg, A-type and low-Ca. These groups are well exposed in the Yalgoo region and their field, geochemical and geochronological characteristics indicate a four-stage magmatic evolution linked with three major phases of juvenile magmatism and greenstone formation. Phase 1 rocks are sparsely preserved and include coeval greenstones and TTGs at 2970–2900 Ma. Phase 2 started with deposition of the Norie and Polelle Group at 2825–2760 Ma, including voluminous sequences of mafic–ultramafic rocks that led to thermal insulation of the crust and vertical crustal reworking with diapiric intrusion of 2760–2740 Ma transitional TTGs and high-Mg granitic rocks (Stage 2). Phase 3 of crustal reworking is associated with the onset of Neoarchean orogenic events in the Murchison Domain and culminated in the intrusion of transitional TTG dykes at c. 2700 Ma during regional east–west shortening (Stage 3). The secular change from TTGs to low-Ca granitic rocks reflects progressive modification of the melting source, from basaltic to granitic, and from deep to shallow melting depths.

In essence, the crustal evolution of the Yalgoo dome at the end of the Archean is an example of in situ formation of felsic continental crust through three phases of juvenile magmatism followed by several melting events that progressively stabilized the continental crust. Although the incremental development of granitic masses is crucial to add buoyancy to the continental crust, the long-term resiliency of Archean cratons was greatly enhanced by their depleted and buoyant mantle keels. These roots protected Archean crust during collisional events and deviated mantle upwelling to the edges of cratons. The development of these lithospheric roots was broadly coeval with crustal growth of Archean cratons, but the minimal exposure of these mantle rocks impedes more accurate correlations of, and deeper insights into, the elusive Archean processes of crust formation and reworking.

Acknowledgements

This work was financially supported by ARC DP11010254. Shachar Lazar is thanked for his assistance and energy during the fieldwork, and the staff at the Carlisle labs for their sample handling.

References

Almeida, JDAC, Dall'Agnol, R, Dias, SB and Althoff, FJ 2010, Origin of the Archean leucogranodiorite–granite suites: evidence from the Rio Maria terrane and implications for granite magmatism in the Archean: Lithos, v. 120, no. 3, p. 235–257.

Amelin, Y, Lee, DC and Halliday, AN 2000, Early-middle Archaean crustal evolution deduced from Lu–Hf and U–Pb isotopic studies of single zircon grains: Geochimica et Cosmochimica Acta, v. 64, no. 24, p. 4205–4225.

Anderson, JL and Smith, DR 1995, The effects of temperature and fO_2 on the Al-in-hornblende barometer: American Mineralogist, v. 80, no. 5–6, p. 549–559.

Arth, JG and Hanson, GN 1975, Geochemistry and origin of the early Precambrian crust of northeastern Minnesota: Geochimica et Cosmochimica Acta, v. 39, no. 3, p. 325–362.

Barker, F and Arth, JG 1976, Generation of trondhjemitic-tonalitic liquids and Archean bimodal trondhjemite-basalt suites: Geology, v. 4, no. 10, p. 596–600.

Bleeker, W 2003, The late Archean record: A puzzle in ca. 35 pieces: Lithos, v. 71, no. 2, p. 99–134.

Boynton, V 1984, Geochemistry of the rare earth elements: Meteorite studies, *in* Rare earth element geochemistry *edited by* P Henderson: Elsevier, Amsterdam, p. 1–510.

Campbell, IH and Hill, RI 1988, A two-stage model for the formation of the granite-greenstone terrains of the Kalgoorlie-Norseman area, Western Australia: Earth and Planetary Science Letters, v. 90, no. 1, p. 11–25.

Campbell, IH, Stepanov, AS, Liang, HY, Allen, CM, Norman, MD, Zhang, YQ and Xie, YW 2014, The origin of shoshonites: new insights from the Tertiary high-potassium intrusions of eastern Tibet: Contributions to Mineralogy and Petrology, v. 167, no. 3, p. 1–22.

Cassidy, KC, Champion, DC, Krapez, B, Barley, ME, Brown, SJA, Blewett, RS, Groenewald, PB, Tyler, IM 2006, A revised geological framework for the Yilgarn Craton, Western Australia: Geological Survey of Western Australia, Record 2006/8, 8p.

Cassidy, KF, Champion, DC, McNaughton, N, Fletcher, IR, Whitaker, AJ, Bastrakova, IV and Budd, A 2002, The characterisation and metallogenic significance of Archaean granitic rocks of the Yilgarn Craton, Western Australia: Minerals and Energy Research Institute of Western Australia (MERIWA), Project no. M281/AMIRA Project no. 482 (unpublished report no. 222).

Champion, DC and Sheraton, JW 1997, Geochemistry and Nd isotope systematics of Archaean granites of the Eastern Goldfields, Yilgarn Craton, Australia: implications for crustal growth processes: Precambrian Research, v. 83, no. 1, p. 109–132.

Champion, DC and Smithies, RH 2001, Archaean granites of the Yilgarn and Pilbara cratons, Western Australia, *in* Proceedings of the Fourth International Archaean Symposium, Perth, Australia 2001 *edited by* KF Cassidy, JM Dunphy, MJ Van Kranendonk: AGSO-Geoscience Australia, Record 2001/37, p. 134–136.

Champion, DC and Smithies, RH 2007, Geochemistry of Paleoarchean granites of the East Pilbara Terrane, Pilbara Craton, Western Australia: implications for Early Archean crustal growth: Developments in Precambrian Geology, v. 15, p. 369–409.

Collins, WJ 1989, Polydiapirism of the Archean Mount Edgar Batholith, Pilbara Block, Western Australia: Precambrian Research, v. 43, no. 1, p. 41–62.

Collins, WJ, Van Kranendonk, AM and Teyssier, C 1998, Partial convective overturn of Archaean crust in the east Pilbara Craton, Western Australia: driving mechanisms and tectonic implications: Journal of Structural Geology, v. 20, no. 9, p. 1405–1424.

Condie, KC 1981, Geochemical and isotopic constraints on the origin and source of Archaen granites: Elsevier, Amsterdam, p. 434.

Condie, KC 1993, Chemical composition and evolution of the upper continental crust: contrasting results from surface samples and shales: Chemical geology, v. 104, no. 1, p. 1–37.

Dall'Agnol, R and de Oliveira, DC 2007, Oxidized, magnetite-series, rapakivi-type granites of Carajás, Brazil: implications for classification and petrogenesis of A-type granites, Lithos, v. 93, no. 3, p. 215–233.

Davis, DW, Amelin, Y, Nowell, GM and Parrish, RR 2005, Hf isotopes in zircon from the western Superior province, Canada: implications for Archean crustal development and evolution of the depleted mantle reservoir: Precambrian Research, v. 140, no. 3, p. 132–156.

Defant, MJ and Drummond, MS 1990, Derivation of some modern arc magmas by melting of young subducted lithosphere: Nature, v. 347, no. 6294, p. 662–665.

Deng, X, Peng, T and Zhao, T 2016, Geochronology and geochemistry of the late Paleoproterozoic aluminous A–type granite in the Xiaoqinling area along the southern margin of the North China Craton: petrogenesis and tectonic implications: Precambrian Research, v. 285, p. 127–146.

Dey, S, Pandey, UK, Rai, AK and Chaki, A 2012, Geochemical and Nd isotope constraints on petrogenesis of granitic rocks from NW part of the eastern Dharwar craton: possible implications for late Archaean crustal accretion: Journal of Asian Earth Sciences, v. 45, p. 40–56.

Dhuime, B, Hawkesworth, CJ, Cawood, PA and Storey, CD 2012, A change in the geodynamics of continental growth 3 billion years ago: Science, v. 335, p. 1334–1336.

Dhuime, B, Wuestefeld, A and Hawkesworth, CJ 2015, Emergence of modern continental crust about 3 billion years ago: Nature Geoscience, v. 8, no. 7, p. 552–555.

Duchesne, JC, Martin, H, Bagiński, B, Wiszniewska, J and Vander Auwera, J 2010, The origin of ferroan-potassic A-type granitic rocks: the case of the hornblende–biotite granite suite of the Mesoproterozoic Mazury complex, northeastern Poland: The Canadian Mineralogist, v. 48, no. 4, p. 947–968.

Eby, GN 1992, Chemical subdivision of the A-type granitic rocks: petrogenetic and tectonic implications: Geology, v. 20, no. 7, p. 641–644.

Farina, F, Albert, C and Lana, C 2015, The Neoarchean transition between medium- and high-K granitic rocks: clues from the Southern São Francisco Craton (Brazil): Precambrian Research, v. 266, p. 375–394.

Fenwick, MJ 2014, Structural evolution of the Yalgoo dome, Yilgarn Craton, Western Australia: a core perspective: Geological Survey of Western Australia, Record 2014/16, 93p.

Fletcher, IR and McNaughton, NJ 2002, Granitoid geochronology: SHRIMP zircon and titanite data, *in* The characterisation and metallogenic significance of Archaean granitoids of the Yilgarn Craton, Western Australia *edited by* KF Cassidy, DC Champion, NJ McNaughton, IR Fletcher, AJ Whitaker, IV Bastrakova and A Budd: Minerals and Energy Research Institute of Western Australia (MERIWA), Project no. M281/AMIRA Project no. 482 (unpublished report no. 222), p. 1–156.

Foley, BJ 1997, Reassessment of Archaean tectonics in the Yalgoo District, Murchison Province, Western Australia: Monash University, Melbourne, BSc thesis (unpublished).

Frost, CD, Frost, BR, Chamberlain, KR and Edwards, BR 1999, Petrogenesis of the 1.43 Ga Sherman batholith, SE Wyoming, USA: a reduced, rapakivi-type anorogenic granite: Journal of Petrology, v. 40, no. 12, p. 1771–1802.

Frost, CD and Frost, BR 2011, On ferroan (A-type) granitic rocks: their compositional variability and modes of origin: Journal of Petrology, v. 52 p. 39–53.

Frost, CD, Frost, BR, Kirkwood, R and Chamberlain, KR 2006, The tonalite–trondhjemite–granodiorite (TTG) to granodiorite–granite (GG) transition in the late Archean plutonic rocks of the central Wyoming Province: Canadian Journal of Earth Sciences, v. 43, no. 10, p. 1419–1444.

Gao, S, Zhang, J, Xu, W and Liu, Y 2009, Delamination and destruction of the North China Craton: Chinese Science Bulletin, v. 54, no. 19, p. 3367–3378.

Geological Survey of Western Australia 2016, Compilation of geochronology information 2016: Geological Survey of Western Australia, digital data package**.**

Griffin, WL, Belousova, EA, Shee, SR, Pearson, NJ and O'Reilly, SY 2004, Archean crustal evolution in the northern Yilgarn Craton: U–Pb and Hf-isotope evidence from detrital zircons: Precambrian Research, v. 131, no. 3, p. 231–282.

Guitreau, M, Blichert-Toft, J, Martin, H, Mojzsis, SJ and Albarède, F 2012, Hafnium isotope evidence from Archean granitic rocks for deep-mantle origin of continental crust: Earth and Planetary Science Letters, v. 337, p. 211–223.

Heilimo, E, Halla, J and Hölttä, P 2010, Discrimination and origin of the sanukitoid series: Geochemical constraints from the Neoarchean western Karelian Province (Finland): Lithos, v. 115, no. 1, p. 27–39.

Ivanic, TJ, Li, J, Meng, Y, Guo, L, Yu, J, Chen, SF, Wyche, S and Zibra, I 2015, Yalgoo, WA Sheet 2241: Geological Survey of Western Australia, 1:100 000 Geological Series.

Ivanic, TJ, Van Kranendonk, MJ, Kirkland, CL, Wyche, S, Wingate, MTD and Belousova, EA 2012, Zircon Lu–Hf isotopes and granite geochemistry of the Murchison Domain of the Yilgarn Craton: evidence for reworking of Eoarchean crust during Meso-Neoarchean plume-driven magmatism: Lithos, v. 148, p. 112–127.

Johnson, TE, Brown, M, Gardiner, NJ, Kirkland, CL and Smithies, RH 2017, Earth's first stable continents did not form by subduction: Nature, v. 543, p. 239–242.

Keller, CB and Schoene, B 2012, Statistical geochemistry reveals disruption in secular lithospheric evolution about 2.5 Gyr ago: Nature, v. 485, no. 7399, p. 490–493.

King, PL, White, AJR, Chappell, BW and Allen, CM 1997, Characterization and origin of aluminous A–type granites from the Lachlan Fold Belt, southeastern Australia: Journal of Petrology, v. 38, no. 3, p. 371–391.

Laurent, O, Martin, H, Moyen, JF and Doucelance, R 2014, The diversity and evolution of late–Archean granitic rocks: evidence for the onset of 'modern-style' plate tectonics between 30 and 25 Ga: Lithos, v. 205, p. 208–235.

Lu, Y, Wingate, MTD, Kirkland, CL and Zibra, I 2017, 209689: metatonalite, Wooley Spring: Geochronology Record 1463: Geological Survey of Western Australia, 4p.

Martin, H 1986, Effect of steeper Archean geothermal gradient on geochemistry of subduction-zone magmas: Geology, v. 14, no. 9, p. 753–756.

Martin, H 1987, Petrogenesis of Archaean trondhjemites, tonalites and granodiorites from eastern Finland: major and trace element geochemistry: Journal of Petrology, v. 28, p. 921–953.

Martin, H, Moyen, JF and Rapp, R 2009, The sanukitoid series: magmatism at the Archaean–Proterozoic transition: Earth and Environmental Science Transactions of the Royal Society of Edinburgh, v. 100 , no. 1–2, p. 15–33.

Martin, H, Smithies, RH, Rapp, R, Moyen, JF and Champion, D 2005, An overview of adakite, tonalite–trondhjemite–granodiorite (TTG), and sanukitoid: relationships and some implications for crustal evolution: Lithos, v. 79, no. 1, p. 1–24.

McDonough, WF and Sun, SS 1995, The composition of the Earth: Chemical Geology, v. 120, no. 3, p. 223–253.

Mikkola, P, Lauri, LS and Käpyaho, A 2012, Neoarchean leucogranitic rocks of the Kianta Complex, Karelian Province, Finland: source characteristics and processes responsible for the observed heterogeneity: Precambrian Research, v. 206, p. 72–86.

Moyen, JF 2011, The composite Archaean grey gneisses: petrological significance, and evidence for a non-unique tectonic setting for Archaean crustal growth: Lithos, v. 123, no. 1, p. 21–36.

Moyen, JF and Martin, H 2012, Forty years of TTG research: Lithos, v. 148, p. 312–336.

Myers, JS and Watkins, KP 1985, Origin of granite–greenstone patterns, Yilgarn Block, Western Australia: Geology, v. 13, no. 11, p. 778–780.

Opiyo-Akech, N, Tarney, J and Hoshino, M 1999, Petrology and geochemistry of granites from the Archaean terrain north of Lake Victoria, western Kenya: Journal of African Earth Sciences, v. 29, no. 2, p. 283–300.

Palin, RM, White, RW and Green, EC 2016, Partial melting of metabasic rocks and the generation of tonalitic–trondhjemitic–granodioritic (TTG) crust in the Archaean: constraints from phase equilibrium modelling: Precambrian Research, v. 287, p. 73–90.

Peng, T, Wilde, SA, Fan, W and Peng, B 2013, Neoarchean siliceous high-Mg basalt (SHMB) from the Taishan granite–greenstone terrane, Eastern North China Craton: petrogenesis and tectonic implications: Precambrian Research, v. 228, p. 233–249.

Prabhakar, BC, Jayananda, M, Shareef, M and Kano, T 2009, Synplutonic mafic injections into crystallizing granite pluton from Gurgunta area, northern part of Eastern Dharwar Craton: implications for magma chamber processes: Journal of the Geological Society of India, v. 74, no. 2, p. 171–188.

Qian, Q and Hermann, J 2013, Partial melting of lower crust at 10–15 kbar: constraints on adakite and TTG formation: Contributions to Mineralogy and Petrology, v. 165, no. 6, p. 1195–1224.

Rapp, RP, Norman, MD, Laporte, D, Yaxley, GM, Martin, H and Foley, SF 2010, Continental formation in the Archean and chemical evolution of the cratonic lithosphere: melt-rock reaction experiments at 3–4 GPa and petrogenesis of Archean Mg-diorites (sanukitoids): Journal of Petrology, v. 51, p. 1237–1266.

Rapp, RP, Shimizu, N, Norman, MD and Applegate, GS 1999, Reaction between slab-derived melts and peridotite in the mantle wedge: experimental constraints at 38 GPa: Chemical Geology, v. 160, no. 4, p. 335–356.

Rey, PF, Philippot, P and Thébaud, N 2003, Contribution of mantle plumes, crustal thickening and greenstone blanketing to the 2.75–2.65 Ga global crisis: Precambrian Research, v. 127, no. 1, p. 43–60.

Shirey, SB and Hanson, GN 1984, Mantle-derived Archaean monozodiorites and trachyandesites: Nature, v. 310, p. 222–224.

Sizova, E, Gerya, T, Stüwe, K and Brown, M 2015, Generation of felsic crust in the Archean: a geodynamic modeling perspective: Precambrian Research, v. 271, p. 198–224.

Skjerlie, KP and Johnston, AD 1992, Vapor-absent melting at 10 kbar of a biotite- and amphibole-bearing tonalitic gneiss: implications for the generation of A-type granites: Geology, v. 20, no. 3, p. 263–266.

Smithies, RH and Champion, DC 2000, The Archaean high-Mg diorite suite: links to tonalite–trondhjemite–granodiorite magmatism and implications for early Archaean crustal growth: Journal of Petrology, v. 41, no. 12, p. 1653–1671.

Smithies, RH, Champion, DC and Van Kranendonk, MJ 2009, Formation of Paleoarchean continental crust through infracrustal melting of enriched basalt: Earth and Planetary Science Letters, v. 281, no. 3, p. 298–306.

Stern, RA and Hanson, GN 1991, Archean high-Mg granodiorite: a derivative of light rare earth element-enriched monzodiorite of mantle origin: Journal of Petrology, v. 32, no. 1, p. 201–238.

Tang, M, Chen, K and Rudnick, RL 2016, Archean upper crust transition from mafic to felsic marks the onset of plate tectonics: Science, v. 351, no. 6271, p. 372–375.

Tatsumi, Y and Ishizaka, K 1981, Existence of andesitic primary magma: an example from southwest Japan: Earth and Planetary Science Letters, v. 53, no. 1, p. 124–130.

Taylor, SR and McLennan, SM 1995, The geochemical evolution of the continental crust: Reviews of Geophysics, v. 33, no. 2, p. 241–265.

Van Kranendonk, MJ, Ivanic, TJ, Wingate, MT, Kirkland, CL and Wyche, S 2013, Long-lived, autochthonous development of the Archean Murchison Domain, and implications for Yilgarn Craton tectonics: Precambrian Research, v. 229, p. 49–92.

Van Kranendonk, MJ, Smithies, RH, Griffin, WL, Huston, DL, Hickman, AH, Champion, DC, Anhaeusser, CR and Pirajno, F 2015, Making it thick: a volcanic plateau origin of Palaeoarchean continental lithosphere of the Pilbara and Kaapvaal cratons: Geological Society, London, Special Publications, v. 389, no. 1, p. 83–111.

Whalen, JB, Currie, KL and Chappell, BW 1987, A-type granites: geochemical characteristics, discrimination and petrogenesis: Contributions to mineralogy and petrology, v. 95, no. 4, p. 407–419.

Whalen, JB, Percival, JA, McNicoll, VJ and Longstaffe, FJ 2004, Geochemical and isotopic (Nd–O) evidence bearing on the origin of late- to post-orogenic high-K granitic rock rocks in the Western Superior Province: implications for late Archean tectonomagmatic processes: Precambrian Research, v. 132 , no. 3, p. 303–326.

Wiedenbeck, M and Watkins, KP 1993, A time scale for granitic rock emplacement in the Archean Murchison Province, Western Australia, by single zircon geochronology: Precambrian Research, v. 61, no. 1, p. 1–26.

Wingate, MTD, Kirkland, CL and Zibra, I 2015a, 155879: granodiorite gneiss, Toben Bore; Geochronology Record 1245: Geological Survey of Western Australia, 4p.

Wingate, MTD, Kirkland, CL, Zibra, I and Wyche, S 2015b, 155822: monzogranite gneiss, Three Mile Well; Geochronology Record 1247: Geological Survey of Western Australia, 3p.

Wingate, MTD, Kirkland, CL and Ivanic, TJ 2014, 207630: porphyritic monzogranite, Garden Pool Well; Geochronology Record 1215: Geological Survey of Western Australia, 4p.

Zhang, C, Holtz, F, Koepke, J, Wolff, PE, Ma, C and Bédard, J 2013, Constraints from experimental melting of amphibolite on the depth of formation of garnet-rich restites, and implications for models of Early Archean crustal growth: Precambrian Research, v. 124, p. 327–341.

Zhang, SB, Zheng, YF, Wu, YB, Zhao, ZF, Gao, S and Wu, FY 2006, Zircon U–Pb age and Hf isotope evidence for 3.8 Ga crustal remnant and episodic reworking of Archean crust in South China: Earth and Planetary Science Letters, v. 252, no. 1, p. 56–71.

Zibra, I, Clos, F, Weinberg, RF and Peternell, M 2017a, The c. 2730 Ma onset of the Neoarchean orogeny in the Yilgarn: Tectonics, v. 36, p. 1787–1813.

Zibra, I, Gessner, K, Smithies, HR and Peternell, M 2014a, On shearing, magmatism and regional deformation in Neoarchean granite–greenstone systems: insights from the Yilgarn Craton: Journal of Structural Geology, v. 67, p. 253–267.

Zibra, I, Peternell, M, Schiller, M, Wingate, MTD, Lu, Y and Clos, F 2017b, Tectono-magmatic evolution of the Neoarchean Yalgoo dome (Yilgarn Craton): diapirism in a pre-orogenic setting: Geological Survey of Western Australia, Report 176, 43p.

Zibra, I, Smithies, RH, Wingate, MTD and Kirkland, CL 2014b, Incremental pluton emplacement during inclined transpression: Tectonophysics, v. 623, p. 100–122.

The Yalgoo dome provides a unique perspective on processes needed to generate an Archean felsic continental crust as all five felsic intrusive groups that typify late Archean terranes are exposed. These five groups can be correlated with three major phases of juvenile magmatism and greenstone formation which caused complete reheating, softening and recycling of the crust. In more than c. 300 Ma, the felsic intrusive magmatism evolution records the secular change from TTGs to low-Ca granitic rocks and reflects the process of stabilization of continental crust through intermittent episodes of enhanced mantle activity and crustal reworking.

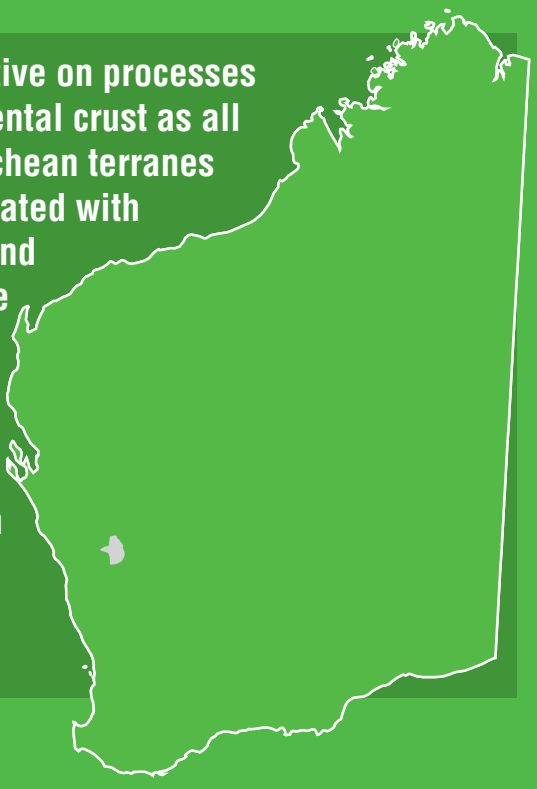

Further details of geological products and maps produced by the Geological Survey of Western Australia are available from:

Information Centre
Department of Mines, Industry Regulation and Safety
100 Plain Street
EAST PERTH WA 6004
Phone: (08) 9222 3459 Fax: (08) 9222 3444

www.dmp.wa.gov.au/GSWApublications

CLOS et al.

BUILDING THE ARCHEAN CONTINENTAL CRUST: 300 Ma OF FELSIC MAGMATISM IN THE YALGOO DOME (YILGARN CRATON)

REPORT 186